Annu. Rev. Astron. Astrophys. 1995. 33:75–113

STELLAR PULSATIONS ACROSS THE HR DIAGRAM: Part 1

Alfred Gautschy

Max-Planck-Institut für Astrophysik, Karl-Schwarzschild-Strasse 1, 85748 Garching, Germany[1]

Hideyuki Saio

Astronomical Institute, Tohoku University, 980 Sendai, Japan

KEY WORDS: stellar physics, stellar evolution

ABSTRACT

Stellar pulsations, either as radial or nonradial dynamical variabilities, are found in many phases of stellar evolution, and these variable stars occupy vastly differing regions on the Hertzsprung-Russell diagram. The diagnostic potential of such oscillations is considerable and its importance will grow in the future when smaller and smaller amplitude variabilities can be monitored as a matter of routine. This review of the theoretical aspects of stellar pulsations appears in two parts. The first part introduces the theoretical concepts and the physical mechanisms involved in stellar pulsations and reviews recent advances therein. Applications of the theory to model neutron-star oscillations and the pulsations of hydrogen-deficient stars are also reviewed.

1. INTRODUCTION

Published attempts to attribute the periodic variation of the light and radial velocity of some variable stars to intrinsic physical mechanisms go back to the second half of the past century (Ritter 1879). The physical theory of stellar pulsations was mainly developed in the first half of the 20th century. The

[1]Current address: Astronomisches Institut der Universität Basel, Venusstrasse 7, CH-4102 Binningen, Switzerland.

0066-4146/95/0915-0075$05.00

expositions of Rosseland (1949, chapter 1) and Ledoux & Walraven (1958) contain very instructive accounts of these early theoretical achievements. However, it was only during the late 1950s to early 1960s (see Zhevakhin 1963 for references to his early contributions; Cox & Whitney 1958; Baker & Kippenhahn 1962, 1965), in connection with the advent of computers, that the driving mechanism behind the oscillations of the most prominent class of pulsating stars—the classical Cepheids—was unraveled. During the following years, the number of publications increased dramatically and our physical understanding of the origin of many types of pulsating variables grew significantly. The review by Cox (1974) provides an excellent impression of the achievements during the 1960s and the early 1970s, in particular of radial pulsation theory. In a concise overview, Smeyers (1984) discusses aspects of nonradial pulsation theory and its application to stellar astrophysics.

Observations of the different classes of pulsating variable stars show that they populate extended regions distributed all over the HR diagram. Possibly, unknown types of pulsating variables are still lurking and will only be discovered with detectors more sensitive than those in use today. In that respect, it is expected (Brown & Gilliland 1994) that, for example, most solar-type stars should also exhibit a solar-like oscillation signature. The technology for detecting and monitoring the expected very weak signals of such oscillations is now under active development.

Figure 1 shows the distribution of a small number of variable stars on the HR diagram. The black dots denote observed stars for which calibrations of their effective temperature and luminosity could be found in the literature; this is possible only for a tiny fraction of all pulsating stars. As the selection is far from complete, the relative density of variable stars on the HR diagram need not be significant. To better link the location of the pulsating variables with stellar structure and evolution, we added some guiding lines from stellar evolution theory in Figure 1. The heavy line stretching from the upper left to the lower right marks the position of the main sequence for solar abundances. Starting at the main sequence are stellar evolutionary tracks of 1, 2, 5, 12, and 30 $M_\odot$ stars, respectively. The horizontal track passing between the paths of the 5 and the 12 $M_\odot$ stars marks the evolution to high temperatures of a post–asymptotic giant-branch (post-AGB) star. Such an object eventually (after the "knee" of its evolutionary track) settles on the cooling track of white dwarfs.

The dotted lines running almost vertically through Figure 1 approximate the location of the "classical" instability strip. In its domain we find (going from high to low luminosities) the Cepheids, RR Lyrae stars, and δ Scuti stars. To avoid overcrowding, they are not labeled separately in Figure 1. Miras (M) and red, long-period variables (SR) are situated at temperatures below the red edge of the instability strip, at luminosities above $\approx 10^3 L_\odot$. The instability strip is extrapolated in an ad hoc manner beyond the main sequence to show

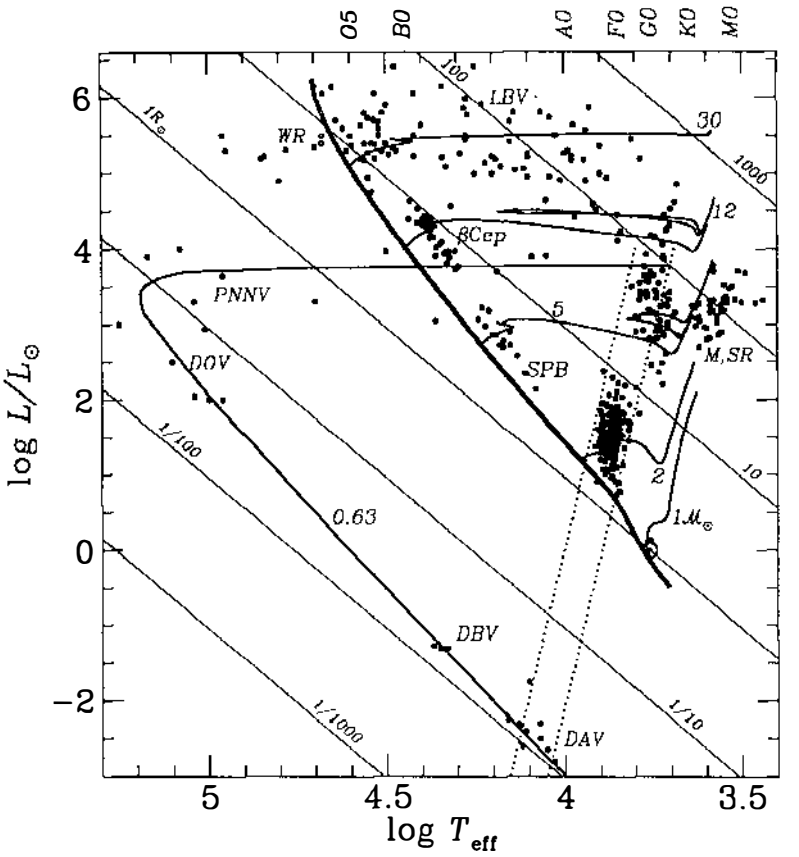

Figure 1 HR diagram showing the distribution of types of pulsating variables (*dots*). The heavy line shows the location of the zero-age main sequence for solar abundances. A number of evolutionary tracks, labeled with the masses in solar units, are included. A post-AGB evolutionary path for a 0.63 $M_\odot$ star is shown; it leaves the AGB at constant luminosity and turns later into a white-dwarf cooling track. The thin diagonal lines represent loci of constant radius. The classical instability strip and its extrapolation towards the white-dwarf region is indicated by dashed lines. Abbreviations: WR: Wolf-Rayet stars; LBV: luminous blue variables; SPB: slowly pulsating B stars; M: Miras; SR: semiregular variables; PNNV: planetary nebulae nuclei variables; DOV, DBV, DAV: variable DO-, DB-, and DA-type white dwarfs.

where it crosses the cooling tracks of white dwarfs. In the neighborhood of this crossing, the pulsating hydrogen-rich DA white dwarfs (ZZ Cet variables) are observed. Along the white dwarfs' cooling tracks, two other oscillating families of white dwarfs are found: the He white dwarfs around $\log T_{\rm eff} = 4.4$ (DB) and the very hot DO white dwarfs situated at the knee of the post-AGB track nearly $L/L_\odot = 3.8$. Along the horizontal part of the post-AGB track, oscillating central stars of planetary nebulae (PNNV) are observed. Also, variable hydrogen-deficient stars show comparable luminosities, with high

effective temperatures exceeding that of the blue edge of the classical instability strip.

The pulsating variables aligning along the main sequence between about 3 and 15 $M_\odot$ are called pulsating B stars; they can be further classified into several subclasses (such as β Cepheids, slowly pulsating B stars, Be stars). The region on the HR diagram above about $10^5 L_\odot$ encompasses the domain where very luminous blue variables (LBV) are observed over a very broad effective-temperature range. Also located at high luminosities are the Wolf-Rayet (WR) stars for which pulsational instabilities might play a role.

Clearly, the study of pulsating stars must not be considered as a narrow-minded domain of research. Pulsational instabilities are encountered in many major phases of stellar evolution, for a large range of stellar masses. Pulsational instabilities provide a unique opportunity to learn about and derive constraints on stellar physical mechanisms that would not be accessible otherwise.

This review will be published in two parts. First, in this volume, we present the theoretical aspects of stellar pulsations and recent advancements therein. We also outline persisting problems that need to be overcome to enable a better understanding of the involved stellar physics. Two aspects of theoretical applications are included: relativistic influences, in particular results from stability investigations of neutron stars; and the pulsations of hydrogen-deficient stars, because their evolutionary state is sufficiently uncertain so that their story can be easily decoupled from Part 2. This second part of the review, to be published in next year's volume, will be restricted to theoretical applications to the different kinds of observed pulsating stars. In it, we will discuss the success of explaining the properties of strongly differing stars within the unified framework of pulsation theory. Again, we will emphasize the limitations and the failures of the theory as it stands today.

As there exists already a number of excellent review articles and textbooks on stellar pulsation theory, we refer to them whenever appropriate. We emphasize physical and astronomical aspects often at the cost of mathematically clean argumentation. For treatises based on more mathematical rigor we suggest Ledoux & Walraven (1958), Cox (1980), Smeyers (1984), or Unno et al (1989). The scope of this exposition prevents us from being encyclopedic. Also, the growing parallel advancement in research fields, together with the inevitable personal bias, often leads to mentioning only exemplary references that might not give proper credit to the creators of underlying ideas.

2. DEVELOPMENTS IN OBSERVATIONAL APPROACHES

The observational emphasis in past decades lay on long-term monitoring of pulsating stars and on the detection of secular variations of their periods. The classes of pulsating stars mentioned in Landoldt-Börnstein (Duerbeck & Seitter 1982) have only one or a very low number of pulsation modes with

amplitudes above a few hundredths of a magnitude. Technological improvements in instrumentation in recent years has lead to a dramatic increase in the availability of high-quality data on pulsating stars, especially measurements of variations with very small amplitudes. Presently, light variations of the order of a few times 10^{-3} mag are monitored as a matter of routine. The requirements of the new discipline of *asteroseismology* (Brown & Gilliland 1994) now drive efforts toward the detection of variations on the level of 10^{-6} mag, which should make possible monitoring of solar-type oscillations in distant stars. Gilliland & Brown (1988) and Gilliland et al (1991) showed differential, simultaneous CCD photometry on one-meter-class telescopes to be sufficient to obtain the highly accurate magnitudes necessary for modern variable star studies. The application of carefully selected statistical methods to ensembles of stars distributed over the field of view of the CCD frame allowed them to reduce the errors to the intrinsic limitations imposed by scintillation and photon statistics. Even under less-than-ideal meteorological conditions, high-quality time-series photometry was still possible. Methodical improvements in reduction strategies to obtain high-quality CCD photometry are being actively pursued (Howell 1992, Kjeldsen & Frandsen 1992). Repeating the success story of solar oscillations for deducing detailed structural information will not be achievable, however, for distant stars as shown by Brown et al (1994) in their estimates of the improvements expected from seismological data for constraining basic stellar parameters such as mass, age, metallicity, or mixing-length parameter.

The detection of very closely spaced oscillation frequencies, like those occurring in rotating, nonradially pulsating stars, requires long time bases over which monitoring has to be essentially uninterrupted to avoid contamination of the power spectra by complicated window functions. One way to avoid the day/night transition problem is to go above the Earth's atmosphere and perform observations on space-borne platforms. A first pilot study—called EVRIS—is planned to fly on the satellite *MARS94* (Baglin et al 1993). Further projects for dedicated photometry and spectroscopy of variable stars on satellites are in preparation (see presentations in GONG92, ITS92). Not only do space-borne experiments allow for long time series, they also eliminate all disturbances induced by the Earth's atmosphere. An easier way to suppress undesired side lobes due to the window function is to coordinate observations of selected variable stars between observatories, optimally distributed in longitude on the Earth. Important observations of oscillating white dwarfs were obtained with this approach by the WET project (Nather et al 1990, Clemens et al 1992). A similar observing strategy devoted to monitoring δ Scuti stars, called STEPHI, has already yielded detailed frequency spectra for several variables (Belmonte et al 1993).

Photometric methods allow the observation only of the large-scale features on the surfaces of stars. Oscillation modes of spherical degree ℓ higher than about 3

(see Section 3.2.1) can potentially be observed by monitoring the variations of spectral line profiles. High signal-to-noise spectroscopy of selected spectral lines provides, through asymmetries and bump features passing through the line profiles, information not only on frequencies but also on the prevailing patterns on the surfaces of oscillating stars (Vogt & Penrod 1983; contributions in ESO90). The moment method (Balona 1986a, b; Aerts et al 1992), together with direct modeling of spectral lines in nonradially oscillating stars (Osaki 1971), can restrict the possible modal admixtures.

To monitor photospheric velocity fields, which are of the order of m sec^{-1} or eventually as small as those encountered in solar oscillations (some 10s of cm sec^{-1}), highly stable and elaborate resonance-type spectrographs are being developed. Their operation is presently still limited to bright stars to obtain sufficiently high signal-to-noise observations on short enough time scales (e.g. Pottasch et al 1992, Mosser et al 1993, Noyes et al 1993, Hatzes & Kürster 1994).

3. THE THEORETICAL MINIMUM[2]

If we want to do better than phenomenologically classify the zoo of stellar pulsations we need know their physical origin. This section addresses the theoretical foundations in a twofold way: We introduce basic notions and concepts for the uninitiated, and we review recent advances in the theoretical treatment of stellar pulsations.

3.1 *Basic Equations*

We reproduce, in a very succinct form, the equations describing the basic physical mechanisms that underlie stellar pulsations. These equations describe self-gravitating fluid configurations whose stability properties are to be investigated. More rigorous, and in particular more pedagogical, derivations can be found in Ledoux & Walraven (1958) or in the monographs of Cox (1980) and Unno et al (1989).

3.1.1 EQUATIONS FOR SELF-GRAVITATING FLUIDS These equations provide the basis for the description of stellar oscillations. The continuity equation may be written as

$$\frac{\partial \rho}{\partial t} + \nabla \cdot (\rho \mathbf{u}) = 0, \tag{1}$$

where ρ denotes the matter density, and $\mathbf{u}$ the fluid velocity field caused by oscillation and/or rotation of the configuration. The momentum equation in an inertial frame of reference reads as

$$\frac{\partial \mathbf{u}}{\partial t} + \mathbf{u} \cdot \nabla \mathbf{u} = -\frac{1}{\rho} \nabla p - \nabla \psi - \langle \mathbf{V} \nabla \cdot \mathbf{V} \rangle, \tag{2}$$

[2]This expression, attributed to LD Landau (Landau & Lifschitz 1981), should paraphrase the minimal conceptual and formal background required to follow the development in a research field.

where p stands for the pressure, ψ for the gravitational potential, and $\mathbf{V}$ for the velocity of turbulent convection. The angle brackets indicate small-scale spatial averages. Poisson's equation for the gravitational potential is

$$\nabla^2\psi = 4\pi G\rho, \tag{3}$$

where G is the gravitational constant. Conservation of thermal energy may be formulated as

$$T\frac{dS}{dt} = \frac{dE}{dt} - \frac{p}{\rho^2}\frac{d\rho}{dt} = \epsilon - \frac{1}{\rho}\nabla\cdot(\mathbf{F}_R + \mathbf{F}_C), \tag{4}$$

where S is the specific entropy, E the specific internal energy, and ϵ the nuclear energy generation rate per unit mass. The energy flux carried by convection is denoted by $\mathbf{F}_C$; $\mathbf{F}_R$ is the radiative flux vector which, in the optically thick regime, is described by diffusion of photons:

$$\mathbf{F}_R = -\frac{4ac}{3\kappa\rho}T^3\nabla T, \tag{5}$$

where a is the radiation constant, c is the speed of light, and κ is the Rosseland mean opacity.

To close the set of equations, an equation of state relating p, ρ, and T needs to be specified. The opacity and the nuclear energy generation rate are assumed to be expressible as functions of ρ, T, and chemical composition. Finally, the quantities related to convection, $\langle\mathbf{V}\cdot\nabla\mathbf{V}\rangle$ and $\mathbf{F}_C$, must be specified. This, the most complicated aspect of the theory (Xiong 1981, Baker 1987, Unno & Xiong 1993), still defies a satisfactory solution. Thus, in most cases the coupling of convection and pulsation is simply neglected. This approximation constrains the success of the theory to stars with weak convection zones only (see also Section 3.3.2).

3.1.2 LINEAR PERTURBATION EQUATIONS To describe the evolution of small perturbations about equilibrium states of stars, linear perturbation equations are used. The linear approximation is the canonical framework in which stability conditions are evaluated and the means by which instability regions on the HR diagram are determined for large sets of stellar models.

The equations describing stellar configurations are conveniently expressed in spherical coordinates (r, θ, ϕ) in which the axis $\theta = 0$ coincides with the axis of possible rotation of the unperturbed star. For simplicity, we assume that only uniform rotation occurs (i.e. $\mathbf{u}_0 = \boldsymbol{\Omega}\times\mathbf{r}$) and that the equilibrium state is axisymmetric. The temporal and azimuthal dependence of any perturbed quantity can then be represented by $\exp[i(\sigma t + m\phi)]$. The perturbation equations derived from Equations (1)–(5) reduce to:

$$\rho' + \nabla\cdot(\rho\boldsymbol{\xi}) = 0, \tag{6}$$

$$-(\sigma + m\Omega)^2\boldsymbol{\xi} + 2\mathrm{i}\,(\sigma + m\Omega)\,(\boldsymbol{\Omega} \times \boldsymbol{\xi}) = -\frac{1}{\rho}\nabla p' + \frac{\rho'}{\rho^2}\nabla p - \nabla\psi' + ((\mathbf{V}\cdot\nabla\mathbf{V}))', \tag{7}$$

$$\nabla^2\psi' = 4\pi G\rho', \tag{8}$$

$$\mathrm{i}\sigma\rho T\delta S = \rho\epsilon\left(\frac{\delta\rho}{\rho} + \frac{\delta\epsilon}{\epsilon}\right) - \delta\,(\nabla\cdot\mathbf{F}_\mathrm{R} + \nabla\cdot\mathbf{F}_\mathrm{C}), \tag{9}$$

and

$$\mathbf{F}'_\mathrm{R} = \mathbf{F}_\mathrm{R}\left(3\frac{T'}{T} - \frac{\kappa'}{\kappa} - \frac{\rho'}{\rho}\right) - \frac{4acT^3}{3\kappa\rho}\nabla T'. \tag{10}$$

The displacement vector $\boldsymbol{\xi}$ is defined as $\mathbf{r} - \mathbf{r}_0$, where the subscript 0 denotes the equilibrium condition. The primed quantities, q', indicate Eulerian perturbations of a physical variable q; δq stands for its Lagrangian perturbations. The two pictures are connected by the relation

$$\delta q = q' + \boldsymbol{\xi}\cdot\nabla q. \tag{11}$$

Together with suitable boundary conditions, Equations (6)–(10) constitute a boundary-eigenvalue problem. The eigenvalue σ is generally a complex quantity, $\sigma_\mathrm{R} + \mathrm{i}\sigma_\mathrm{I}$, where σ_R represents the oscillation frequency and σ_I measures the growth ($\sigma_\mathrm{I} < 0$) or damping ($\sigma_\mathrm{I} > 0$) time.

3.2 *Adiabatic Pulsations*

In the adiabatic approximation, fluid parcels displaced by an oscillation do not exchange energy with their surroundings. Such an assumption is very good for many stellar oscillations and it applies in a star if the dynamical perturbation time is much shorter than the time for heat exchange. In the adiabatic approach, which is also occasionally referred to as an *isentropic* approximation (Smeyers 1984), the relation

$$\frac{\delta\rho}{\rho} = \frac{1}{\Gamma_1}\frac{\delta p}{p} \tag{12}$$

applies. The adiabatic exponent Γ_1 is defined by $\Gamma_1 \equiv (\partial \ln p/\partial \ln \rho)_\mathrm{S}$. In the adiabatic approximation, the dynamical equations of stellar pulsations decouple from the energy conservation and flux equations (Equations 9 and 10). Only for this simplified problem do we presently have mathematical theorems specifying its properties.

3.2.1 RADIAL AND NONRADIAL PULSATIONS The equation for the displacement vector field in a nonrotating, spherically symmetric star (we neglect the influence of turbulent convection in the following) may be written symbolically as

$$-\sigma^2\boldsymbol{\xi} + \boldsymbol{\mathcal{L}}(\boldsymbol{\xi}) = 0, \tag{13}$$

where $\mathcal{L}$ is a Hermitian operator in the case of vanishing pressure at the stellar surface. (Even for real stars having finite, but small surface pressure, Hermiticity remains approximately true.) The explicit form of $\mathcal{L}$ is given in section 15.2 of Cox (1980). Recently, Beyer & Schmidt (1994) elaborated on mathematical subtleties concerning the eigen-spectrum of self-adjoint problems when both boundaries of the operator $\mathcal{L}$ are singular. They found that no additional, continuous mode spectrum exists under these conditions, as had been suspected for a long time (Ledoux & Walraven 1958). Because $\mathcal{L}$ is Hermitian, all eigenvalues σ^2 are real and eigenfunctions associated with different eigenvalues are orthogonal to one another. The reality of σ^2 ensures that the temporal behavior of the adiabatic perturbations is purely oscillatory when $\sigma^2 > 0$ and monotonic when $\sigma^2 < 0$ (dynamical instability).

We may decompose the term $\mathcal{L}(\boldsymbol{\xi})$ in Equation (13) into the form

$$\mathcal{L}(\boldsymbol{\xi}) = f_1 \hat{\mathbf{e}}_r + \nabla f_2, \tag{14}$$

where $\hat{\mathbf{e}}_r$ is the unit vector in the radial direction, and f_1 and f_2 consist of terms proportional to ξ_r or $\nabla_\perp \cdot \boldsymbol{\xi}_\perp$, with

$$\boldsymbol{\xi}_\perp \equiv \xi_\theta \hat{\mathbf{e}}_\theta + \xi_\phi \hat{\mathbf{e}}_\phi$$

and

$$\nabla_\perp \equiv \hat{\mathbf{e}}_\theta \frac{\partial}{\partial \theta} + \frac{\hat{\mathbf{e}}_\phi}{\sin\theta} \frac{\partial}{\partial \phi}.$$

When this decomposition is applied to Equation (13), only angular derivatives in the form of $\nabla_\perp^2$ occur. As the spherical harmonics $Y_\ell^m(\theta, \phi)$ are eigenfunctions of the operator $\nabla_\perp^2$, i.e.

$$\nabla_\perp^2 Y_\ell^m(\theta, \phi) = -\ell(\ell + 1) Y_\ell^m(\theta, \phi), \tag{15}$$

the angular dependencies of perturbed quantities can be expressed by a *single* $Y_\ell^m(\theta, \phi)$. Perturbed scalar variables are directly proportional to Y_ℓ^m. The displacement vector for a *spheroidal* mode is decomposed as

$$\boldsymbol{\xi} = \left[\xi_r \hat{\mathbf{e}}_r + \xi_h \left(\hat{\mathbf{e}}_\theta \frac{\partial}{\partial \theta} + \hat{\mathbf{e}}_\phi \frac{1}{\sin\theta} \frac{\partial}{\partial \phi} \right) \right] Y_\ell^m(\theta, \phi) e^{i\sigma t}. \tag{16}$$

The equations describing the dynamical behavior of nonradial motions are thus reduced to an ordinary differential equation with radial dependence only. (This property holds also in the case of nonadiabatic oscillations, see e.g. Unno et al 1989, section 13.) For vector-valued quantities, the direct use of vector spherical harmonics might prove preferable. Takata & Shibahashi (1994) introduced them to simplify the evaluation of the Lorentz- and Coriolis-force terms in a perturbation analysis of oscillations in magnetized, rotating stars.

The effects of the angular dependence of the eigenfunctions enter the equations only through terms proportional to $\ell(\ell+1)$, which is related to the horizontal wavenumber of the oscillation, $[\ell(\ell+1)]^{1/2}/r$. Because the *azimuthal order* m ($-\ell \leq m \leq \ell$) does not appear in the equations, the eigenvalues (i.e. oscillation frequencies) are $(2\ell+1)$-fold degenerate. The quantity ℓ is referred to as the *spherical degree* of a mode. The different radial overtones, i.e. different numbers of nodes (n or k) of the eigenfunctions in radial direction, are called *radial orders*.

Inspection of Equations (13) and (14) shows that these equations are also satisfied if

$$\sigma = 0, \quad \xi_r = 0, \quad \text{and} \quad \nabla_\perp \cdot \boldsymbol{\xi}_\perp = 0.$$

The last two relations are satisfied when the displacements are *toroidal*, i.e. when

$$\boldsymbol{\xi} \propto \nabla_\perp \times (\hat{\mathbf{e}}_r Y_\ell^m). \tag{17}$$

The eigenfrequency is zero for vanishing rotation or vanishing magnetic field as toroidal displacements on spherical shells of a fluid induce only a translation of the spherical equilibrium structure. If the star rotates, toroidal displacements describe Rossby waves with finite oscillation frequencies.

Oscillations with $\ell = 0$ represent spherically symmetric, i.e. radial pulsations. In this case, Equation (13) is reduced to

$$-\sigma^2 \xi_r - \frac{1}{r^4 \rho}\left(\Gamma_1 p r^4 \frac{d\xi_r}{dr}\right) - \frac{1}{\rho r}\left\{\frac{d}{dr}[(3\Gamma_1 - 4)p]\right\}\xi_r = 0. \tag{18}$$

This equation, together with boundary conditions ($\xi_r = 0$ at the center and, for example, $\delta p = 0$ at the surface), form a Sturm-Liouville-type eigenvalue problem with eigenvalue σ^2. The eigenvalue associated with the eigenfunction having n nodes is represented by σ_n^2. The eigenvalues form a Sturmian sequence, $\sigma_0^2 < \sigma_1^2 < \sigma_2^2 < \ldots$. Thus, the period of oscillation decreases as the number of nodes increases because the period is approximately the sound travel time between two adjacent nodes (Hansen 1972).

From the above equation and the variational property of the eigenvalues, the inequalities

$$(3\langle\Gamma_1\rangle - 4)(-E_{\text{grav}}/I) > \sigma_0^2 > (3\langle\Gamma_1\rangle - 4)4\pi G\langle\rho\rangle/3$$

can be derived. Here, $\langle\rho\rangle$ is the mean density of the star, $\langle\Gamma_1\rangle$ an average of the adiabatic exponent Γ_1, E_{grav} the gravitational potential energy, and I the moment of inertia of the star. (See sections 8.9 and 8.10 in Cox 1980 for a derivation and discussion). If $\langle\Gamma_1\rangle < 4/3$, at least the fundamental mode is dynamically unstable ($\sigma_0^2 < 0$). We note that, since $(-E_{\text{grav}}/I)$ is proportional to the mean density of the star, the period of the fundamental mode $(2\pi/\sigma_0)$ is inversely proportional to the square of the mean density. This dependence states the period–mean density relation of stellar pulsations.

3.2.2 ASYMPTOTIC BEHAVIOR The asymptotic behavior of nonradial pulsations provides insight into the nature of the elementary modal families in the limit of high and low oscillation frequencies, respectively. To keep the discussion simple, we disregard the Eulerian perturbation of the gravitational potential ψ' (Cowling approximation) in this subsection (Cowling 1941). This approach is particularly suitable for high-order modes. Using (16), the continuity and momentum equations are written as

$$\frac{1}{r^2}\frac{d}{dr}(r^2\xi_r) - \frac{g}{c_s^2}\xi_r + \left(1 - \frac{L_\ell^2}{\sigma^2}\right)\frac{p'}{\rho c_s^2} = 0 \tag{19}$$

and

$$\frac{1}{\rho}\frac{dp'}{dr} + \frac{g}{\rho c_s^2}p' + (N^2 - \sigma^2)\xi_r = 0. \tag{20}$$

L_ℓ and N are, respectively, the *Lamb frequency* and the *Brunt-Väisälä frequency* defined as

$$L_\ell \equiv \sqrt{\frac{\ell(\ell+1)c_s^2}{r^2}} \quad \text{and} \quad N = \sqrt{g\frac{\delta}{c_p}\frac{dS}{dr}}, \tag{21}$$

where g is the local gravitational acceleration, c_s is the adiabatic sound speed, c_p is the specific heat, and $\delta = \partial \log \rho / \partial \log T$, both at constant pressure.

The two frequencies given in Equation (21) play important roles in characterizing nonradial oscillations. This can be seen in a local analysis where we assume that

$$\xi_r,\ p' \propto \exp(ik_r r),$$

if $|k_r| \gg 1$. Upon substituting this decomposition attempt into Equations (19) and (20), we obtain the dispersion relation

$$k_r^2 \simeq \frac{(\sigma^2 - L_\ell^2)(\sigma^2 - N^2)}{\sigma^2 c_s^2}. \tag{22}$$

An oscillation propagates in radial direction (i.e. it oscillates spatially) when k_r is real. If L_ℓ and N vary appropriately in space, the oscillations are well trapped within their propagation regions. The dispersion relation shows that two types of oscillation are possible: a p-mode, which is a propagating wave when $\sigma^2 > L_\ell^2$ and $\sigma^2 > N^2$; and a g-mode, which propagates when $\sigma^2 < L_\ell^2$ and $\sigma^2 < N^2$. The propagation zones from a short-wave analysis are indicated by dotted regions, denoted by P and G, in Figure 2. (See also Section 3.2.3 for explanations of Figure 2.) In all other cases, the oscillation amplitude decays exponentially in space; the oscillation is evanescent. In the high-frequency limit of p-modes, k_r grows as σ^2/c_s^2, while it is proportional to $\ell(\ell+1)N^2/(\sigma r)^2$ for very-low frequency g-modes. The restoring force for the p-modes comes from the compressibility of the gas. Thus, p-modes are, as the radial pulsations,

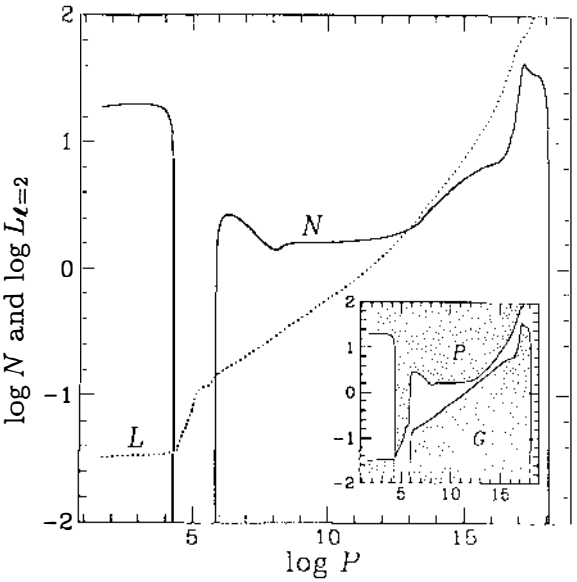

Figure 2 (*Large graph*) Spatial run of the Lamb frequency $L_{\ell=2}$ and of the Brunt-Väisälä frequency N (*solid line*) in a star. The model represents a 2 $M_\odot$ star in its subgiant stage (model for a δ Scuti variable). The ordinate is expressed in units of the free-fall time; the abscissa shows the total pressure (in cgs units) inside the star. The stellar surface is on the left; the stellar center is on the right. (*Inset*) The propagation regions, indicated by the dotted areas, for p- and g-modes (labeled as P and G region, respectively), derived from an explicit short-wave analysis. The propagation regions are well approximated by the inequalities involving Lamb and Brunt-Väisälä frequencies given in the text.

sound waves influenced by the gravitational field of the star. On the other hand, the restoring force for the g-modes is the buoyancy force, which works only for nonspherically symmetric perturbations.

In a simple stellar model such as a zero-age main-sequence model, the eigenfrequency domain of p-modes is well separated from and lies at larger values than the eigenfrequency range of g-modes. The Lamb frequency for a given value of ℓ decreases monotonically outward, while the Brunt-Väisälä frequency increases outward. At some zone in the star, these two frequencies coincide. This frequency level approximately separates the p-mode and g-mode frequency domains: Modes with higher frequencies are p-modes; those with lower frequencies are g-modes. The propagation zone of p-modes is in the envelope; g-modes propagate in the core regions, at least for main-sequence stars. For white dwarfs the roles of the p- and g-modes are exchanged. Between the lowest-order g- and p-modes ($n = 1$) for a given degree ℓ (larger than one) there exists an f-mode whose eigenfunction has no node in the radial direction (see figure 17.2 in Cox 1980 or figure 14.1 in Unno et al 1989). Nodes may appear, however, in centrally concentrated models.

As the central concentration of a star increases during its evolution, the Brunt-Väisälä frequency in the core and hence the eigenfrequencies of g-modes increase. When the frequency of a g-mode approaches and exceeds the frequency of the f- or a p-mode, the two frequencies undergo an "avoided crossing" (see Figure 3 and Section 3.2.3), because two different modes with the same ℓ cannot have the same frequency. In evolved stars, the frequency range of the g-modes overlaps the one of the p-modes. Any mode whose frequency is in this overlapping range has two propagation zones; it propagates as a p-mode in the envelope and as a g-mode in the deep interior. Although such a mode has dual character its overall character may be dominated by the propagation zone that traps more pulsation energy.

In far-evolved stars, the Brunt-Väisälä frequency is very large in the core and for any nonradial pulsation with a moderate frequency, $N^2 \gg \sigma^2$ in the deep interior. Thus, the radial wavenumber k_r is huge there, meaning that the eigenfunction oscillates rapidly in space. Because the short wavelength of this spatial oscillation causes thermal dissipation of pulsation energy, such nonradial oscillations are unlikely to be excited in a giant star.

For oscillations of large radial order n and small spherical degree, asymptotic formulations were derived (Vandakurov 1968, Tassoul 1980, Smeyers & Tassoul 1987):

$$\sigma \approx \pi(n + \ell/2) \left(\int_0^R \frac{1}{c_s} dr \right)^{-1} \tag{23}$$

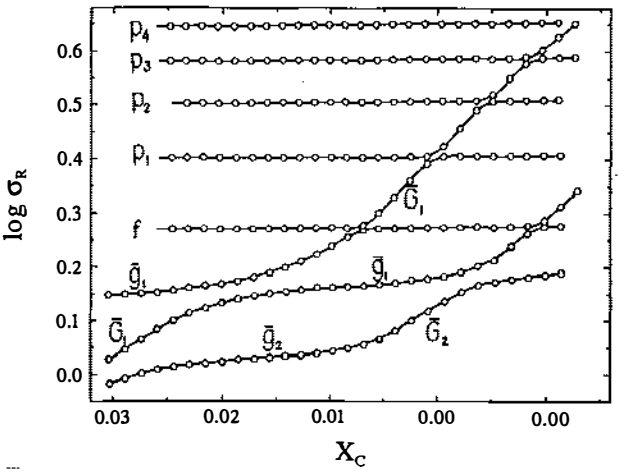

Figure 3 Behavior of the oscillation frequencies of a 12 $M_\odot$ star evolving off the main sequence. Time is parameterized by the central hydrogen content X_C on the abscissa. Avoided crossings are induced by the growing frequencies of the $\overline{G}_n$ modes (see text) during central contraction.

for p-modes and

$$\sigma \approx \frac{[\ell(\ell+1)]^{1/2}}{n\pi} \int_{r_a}^{r_b} \frac{N}{r}\, dr \tag{24}$$

for g-modes, where $N^2 > 0$ in the zone $r_a < r < r_b$. For high-order p-modes, it is the separation of the *frequencies* that becomes equidistant, whereas for the g-modes it is the *periods* ($= 2\pi/\sigma$) that approach an equidistant separation.

An extension of the second-order expansions relying on the Cowling approximation to fourth order was presented by Roxburgh & Vorontsov (1994b). Tassoul (1990) and Vorontsov (1992) presented second-order asymptotic analyses for p-modes, including the Eulerian perturbation of the gravitational potential. For numerical calculations, Bernstein et al (1992) suggested an interesting method to compute solutions to eigenvalue problems with rapidly oscillating eigensolutions. The "small frequency separation," $\sigma_{\ell,n} - \sigma_{\ell+2,n-1}$, whose asymptotic behavior plays an important role in seismic investigations was physically discussed by Van Hoolst & Smeyers (1991) and Roxburgh & Vorontsov (1994a).

The asymptotic properties of the nonradial eigenvalue problem has found extensive application in recent years. Gough & Toomre (1991) reviewed aspects in connection with solar seismology and Brown & Gilliland (1994) elaborated on the use of asymptotic theory in asteroseismology mainly of solar-type stars and of white dwarfs.

3.2.3 MODE COUPLING In a simple stellar model with no pronounced central concentration, as in zero-age main-sequence stars, a single propagation zone ("cavity") exists for a g- or p-mode. Thus, a horizontal line in a propagation diagram, i.e. at a selected oscillation frequency, passes through only one propagation region, either through a P- or a G-region (dotted regions in inset of Figure 2). In evolved stars with high density contrast, however, the Brunt-Väisälä frequency is high in the core and at its outer edge (in the μ-gradient zone where the molecular weight of the stellar matter changes due to nuclear transmutations) so that two or more propagation zones, separated by evanescent zones, develop (see Figure 2). Therefore, oscillation modes can have dual character: They propagate with p-mode properties in the envelope and they assume g-mode character in the deep interior.

Each oscillation mode has usually a main cavity wherein most of the oscillation energy is confined, even if the mode has more than one propagation zone. In such cases, it appeared convenient to classify modes according to their properties in the main cavity (Shibahashi & Osaki 1976). For example, $\overline{g}_n$ ($\overline{p}_n$) modes are trapped in a G-cavity (P-cavity), which has n nodes. Modes trapped in the G-cavity of the μ-gradient zone are denoted as $\overline{G}_n$.

The oscillation energy density decays exponentially in evanescent regions, while it stays constant in propagation regions. Hence, the thicker the evanes-

cent zones are in mass between neighboring propagation regions, the better is the trapping of oscillation energy in a particular cavity. Since the evanescent zone between the P-cavity in the envelope and the G-cavity in the μ-gradient zone is thicker for higher-ℓ modes, the distinction between $\overline{G}_n$, $\overline{g}_n$, and $\overline{p}_n$ is more pronounced for high-ℓ modes.

As a star evolves, its eigenfrequencies adapt to the variation of the Brunt-Väisälä frequency (g-modes) or the Lamb frequency (p-modes). In the μ-gradient zone at the outer edge of the core, the Brunt-Väisälä frequency gradually increases during the main-sequence evolution causing the eigenfrequencies of the $\overline{G}_n$ modes (see Figure 3 adopted from Gautschy 1992) to rise.

Two modes with the same ℓ but different main cavities behave essentially independently unless their eigenfrequencies happen to be close to each other. From Figure 3 it is clear that the $\overline{G}_n$ and the $\overline{p}_m$ modes do not have equal eigenfrequencies at any evolutionary phase. They undergo an avoided crossing in the modal diagram[3] shown in Figure 3. At closest approach, the oscillation energy of a mode is partitioned between the P-cavity in the envelope and the μ-gradient G-cavity. Hence, the distinction between the physical properties of the two modes is less prominent. Modes at such a stage may be regarded as coupled, both being composed of a g-mode part from the μ-gradient zone and a p-mode part from the envelope. By artificially suppressing one of the cavities in calculating the eigenfrequencies, Aizenman et al (1977) showed that the picture of coupling eigenmodes of different cavities indeed applies. Avoided crossings were first found by Osaki (1975) in massive main-sequence star evolution.

An asymptotic analysis of nonradial oscillations casts additional light on the relation between the avoided crossing and mode coupling and reveals that the avoided crossing is only one possibility of unfolding of eigenfrequencies during a close encounter. For an eigenmode with frequency σ propagating in two cavities, its dispersion relation, satisfying appropriate boundary conditions, can be written as

$$\mathcal{D}_1(\sigma)\mathcal{D}_2(\sigma) = \epsilon \tag{25}$$

(Shibahashi 1979, section 16 in Unno et al 1989), where ϵ is a small positive number that decreases exponentially with increasing thickness of the evanescent zone between the two cavities. For $\epsilon = 0$, Equation (25) is satisfied when $\mathcal{D}_1(\sigma) = 0$ or $\mathcal{D}_2(\sigma) = 0$. Let $\overline{\sigma}_1$ and $\overline{\sigma}_2$ be the oscillation frequencies satisfying (25) for $\epsilon = 0$. Each of these frequencies corresponds to an oscillation mode whose energy is exclusively confined to one of the two cavities. Thus, for $\epsilon = 0$ the two modes are independent of each other.

When the frequencies of modes of different cavities happen to come close to each other, coupling between the two modes becomes important if the

[3]For a *modal diagram* we designate representations of oscillation frequencies versus some control parameter describing the model sequence. In Figure 3, the central hydrogen content is a suitable monotonous variable to parameterize time evolution.

evanescent region separating the two cavities is not too thick. We write the oscillation frequency σ of the coupled system as

$$\omega = d + \overline{\sigma}_1 = d + \overline{\sigma}_2 + \Delta,$$

where $\Delta \equiv \overline{\sigma}_1 - \overline{\sigma}_2$. Here we consider the case where $|d|, |\Delta| \ll \overline{\sigma}_1, \overline{\sigma}_2$. Substituting these expressions into Equation (25) and solving with respect to d, leads to

$$d_\pm = -\frac{\Delta}{2} \pm \sqrt{\frac{\Delta^2}{4} + \frac{\epsilon}{(\partial \mathcal{D}_1/\partial\sigma)(\partial \mathcal{D}_2/\partial\sigma)}}.$$

If $(\partial \mathcal{D}_1/\partial\sigma)(\partial \mathcal{D}_2/\partial\sigma)$ is positive, $d_\pm$ takes purely real values. In this case, the mode coupling ($\Delta \to 0$) appears as an avoided crossing with two modes having slightly different real eigenfrequencies. On the other hand, if $(\partial \mathcal{D}_1/\partial\sigma)$ $(\partial \mathcal{D}_2/\partial\sigma)$ is negative and Δ is sufficiently small, $d_\pm$ and hence the frequencies assume complex values that are complex conjugate to each other.

The quantity $\partial \mathcal{D}/\partial\sigma$ can be shown to be proportional to the energy of oscillation (Cairns 1979, Lee & Saio 1990b). Therefore, an avoided crossing appears when an oscillation mode having positive (negative) energy encounters another mode with positive (negative) energy, while a complex conjugate pair (instability band) appears if one mode has positive energy and the other has negative energy. All the g^+- and p-modes were shown to have positive energies (Lee & Saio 1990b), which means that coupling among these modes can generate only avoided crossings.

In a rotating convective core, a g^--mode can be stabilized to become purely oscillatory. Such a mode has negative energy and, in a mode coupling with a g^+-mode of the radiative envelope (Lee & Saio 1989, 1990b), can cause complex conjugate eigenfrequencies. Such instability bands resulting from mode interactions also occur in differentially rotating cylinders (Glatzel 1987) and in stellar pulsations using the nonadiabatic reversible (NAR) approximation (Gautschy & Glatzel 1990).

3.2.4 PULSATIONS IN ROTATING STARS Here we considered pulsations in rotating stars in the adiabatic approximation only. Equations (6)–(8) are combined to give

$$-(\sigma + m\Omega)^2\boldsymbol{\xi} + 2i(\sigma + m\Omega)\boldsymbol{\Omega} \times \boldsymbol{\xi} + \boldsymbol{\Omega} \times (\boldsymbol{\Omega} \times \boldsymbol{\xi}) + \mathcal{L}(\boldsymbol{\xi}) = 0. \qquad (26)$$

Although we restrict ourselves to uniform rotation, the above equation applies also to differentially rotating stars. By taking the scalar product with $\boldsymbol{\xi}^*$ and integrating over the whole volume we obtain

$$-(\sigma + m\Omega)^2 a + (\sigma + m\Omega)b + c = 0, \qquad (27)$$

where

$$a \equiv \int_V \boldsymbol{\xi}^* \cdot \boldsymbol{\xi} \rho \, d^3\mathbf{x},$$

$$b \equiv 2i \int_V \boldsymbol{\xi}^* \cdot (\boldsymbol{\Omega} \times \boldsymbol{\xi}) \rho \, d^3\mathbf{x},$$

and

$$c \equiv \int_V \boldsymbol{\xi}^* \cdot [\mathcal{L}(\boldsymbol{\xi}) + \boldsymbol{\Omega} \times (\boldsymbol{\Omega} \times \boldsymbol{\xi})] \rho \, d^3\mathbf{x}.$$

The quantities a, b, and c were proved to be real by Lynden-Bell & Ostriker (1967). Solving the above equation we obtain

$$\sigma + m\Omega = \frac{1}{2a}(b \pm \sqrt{b^2 + 4ac}). \tag{28}$$

For a nonrotating star ($\Omega = 0$), Equation (28) reduces to

$$\sigma = \pm\sqrt{\frac{c}{a}} \equiv \pm\sigma_0.$$

Note that the sign of the frequency is not physically important as it changes the phase of pulsation only. For slow rotation ($\sigma_0 \gg \Omega$), $4ac \gg b^2$ so that we can expand:

$$\sigma = \pm\sqrt{\frac{c}{a}} + \frac{1}{2}\frac{b}{a} - m\Omega + O(\Omega^2) = \pm\sigma_0 - m\Omega(1 - C_{n,\ell}) + O(\Omega^2).$$

Thus, rotation lifts the $(2l + 1)$-fold degeneracy of the eigenfrequencies completely. The coefficient $C_{n,\ell}$ is an integral quantity determined by the stellar structure and the eigenfunction of the oscillation mode; its magnitude is usually much less than unity. Second-order effects were studied by Saio (1981) and Martens & Smeyers (1986) for uniform rotation, and by Dziembowski & Goode (1992) for differential rotation.

When the rotation frequency Ω is comparable to or larger than σ_0, which is to be expected for high-order g-modes, eigenfunctions and eigenvalues are considerably modified compared to those in nonrotating stars and new features arise (see chapter VI in Unno et al 1989 or see Saio & Lee 1991). A special case is the toroidal displacements, characterized by Equation (17). For them, $c = \mathcal{O}(\Omega^3)$ and hence $\sigma_0 = 0$. In consequence, Equation (24) leads to

$$\sigma + m\Omega = \begin{cases} 0 & \text{or} \\ 2m\Omega/[\ell(\ell+1)]. \end{cases}$$

The next higher terms are of the order Ω^3 (see Papaloizou & Pringle 1978, Provost et al 1981). The lower case corresponds to a global Rossby or planetary wave.

3.2.5 EFFECTS OF MAGNETIC FIELDS The effects of magnetic fields are usually treated as small perturbations applied in addition to the conventional adiabatic hydrodynamic oscillation problem. Such a procedure applies whenever the magnetic pressure remains much smaller than the gas pressure over the domain of the eigenvalue problem. Such conditions are easily fulfilled deep in the interior of stars but can break down, even for moderate magnetic fields, close to the surface.

In the presence of a magnetic field, the momentum equation (2) acquires an additional term owing to the Lorentz force. The linearized form is

$$\sigma^2 \boldsymbol{\xi} = -\frac{\rho'}{\rho^2}\nabla p + \nabla\psi' + \frac{1}{\rho}\nabla p' - \frac{1}{4\pi\rho}[(\nabla \times \mathbf{B}') \times \mathbf{B} + (\nabla \times \mathbf{B}) \times \mathbf{B}']. \tag{29}$$

In the magnetohydrodynamic approximation and assuming perfect conduction in the plasma, the perturbed magnetic field is determined by

$$\mathbf{B}'(\mathbf{r}) = \nabla \times (\boldsymbol{\xi} \times \mathbf{B}_0)\,.$$

Most of the formal difficulties arise from the specification of the spatial configuration of $\mathbf{B}_0$. Particularly laborious expressions arise for non-force-free magnetic fields (Goosens 1972, Goosens et al 1976) that deform the equilibrium structure. Another source of complexity comes from magnetic axes that are inclined relative to the coordinate system in which the nonradial modes are expanded.

To find corrections to adiabatic eigenfrequencies of nonmagnetized configurations by the influence of a magnetic field, either direct perturbation methods (Ledoux & Simon 1957, Unno et al 1989) or variational treatments are used (Kovetz 1966, Nasiri & Sobuti 1989). In contrast to the rotational influence, magnetic fields of axisymmetric configuration remove m-degeneracy only partially as only m^2 terms enter the lowest-order perturbation expressions. Hence, an eigenfrequency $\sigma_{n,\ell}$ of a nonrotating, nonmagnetized star acquires $\ell + 1$ components by the presence of a magnetic field. In contrast to the perturbing influence of rotation, magnetic fields also shift the $m = 0$ component of the eigenfrequency. Generally, g-modes experience stronger frequency shifts than the p-modes do in $\mathbf{B}$-fields. For arbitrarily aligned axes of magnetic fields or of rotation in the coordinate system in which nonradial modes are expanded the m-degeneracy can be lifted completely (Goode & Thompson 1992) when observed by an inertial observer.

The perturbation approach has been widely used and extended during the past few years, particularly for solar-oscillation analyses (Gough & Thompson 1990, Goode & Thompson 1992). A detailed analysis of the combined effects of rotation and magnetic fields has been done in a study of rapidly oscillating

Ap stars by Shibahashi & Takata (1993). Jones et al (1989) performed a feasibility study to detect weak [$\bullet(10^5$ G)] magnetic fields by their traces in the oscillation spectra of white dwarfs.

3.3 *Excitation Mechanisms*

To discuss the excitation mechanisms of pulsations we use, for the sake of simplicity, the quasi-adiabatic approximation in which the entropy perturbation is evaluated from Equation (9) using the adiabatic relation (12) and adiabatic eigenfunctions. This approximation provides reasonable results only when nonadiabaticity is small.

After some manipulation of Equations (6)–(8) and (12), we obtain

$$\frac{dE_W}{dt} = \int_0^M \delta T \frac{d\delta S}{dt} dM_r = \int_0^M \delta T \, \delta \left[\epsilon - \frac{1}{\rho} \nabla \cdot (\mathbf{F}_R + \mathbf{F}_C) \right] dM_r, \quad (30)$$

where

$$E_W = \frac{1}{2} \int \left[(\mathbf{u}')^2 + \left(\frac{p'}{\rho c_s} \right)^2 + \frac{g^2}{N^2} \left(\frac{p'}{\Gamma_1 \rho} - \frac{\rho'}{\rho} \right)^2 + \frac{\rho'}{\rho} \psi' \right] dM_r, \quad (31)$$

which represents the kinetic and potential energy of the pulsation. (In deriving the above equations we disregarded the effect of rotation and convection in the momentum equation.) Equation (30) measures the change of the pulsation energy by the modulation of the nuclear energy generation rate and of the energy flux.

After integrating over a pulsation cycle, the work integral (30) takes the form

$$W = \oint \frac{dE_W}{dt} dt = \frac{\pi}{\sigma} \int_0^M \left[\frac{\delta T_r}{T} \delta \epsilon_r - \frac{\delta T_r}{T} \delta \left(\frac{1}{\rho} \nabla \cdot \mathbf{F}_R \right)_r - \frac{\delta T_r}{T} \delta \left(\frac{1}{\rho} \nabla \cdot \mathbf{F}_C \right)_r \right] dM_r, \quad (32)$$

where the temporal and angular dependencies of perturbed quantities q are factorized as

$$\delta q = Re[\delta q_r Y_\ell^m e^{i\sigma t}].$$

The real part of the indicated quantity is denoted by $Re(\ldots)$. The subscript r is added to indicate that the quantity is a function of r only. All quantities with subscript r are real by the use of the quasi-adiabatic approximation. If W is positive the pulsation energy grows during one pulsation cycle, i.e. the pulsation is excited (or overstable).

3.3.1 ϵ-MECHANISM The first term on the right-hand side of Equation (32) describes the driving by the ϵ-mechanism, i.e. by the effects of the temperature

and density dependence of nuclear burning. After some manipulation, we can write

$$\int_0^M \frac{\delta T_r}{T}\,\delta\epsilon_r\,dM_r = \int_0^M \epsilon\left(\epsilon_T + \frac{\epsilon_\rho}{\Gamma_3 - 1}\right)\left(\frac{\delta T_r}{T}\right)^2 dM_r, \tag{33}$$

where $\epsilon_T = (\partial \ln \epsilon/\partial \ln T)_\rho$ ($\approx$ 4–30), $\epsilon_\rho = (\partial \ln \epsilon/\partial \ln \rho)_T$ ($\approx$ 1–2), and $\Gamma_3 - 1 \equiv (\partial \ln T/\partial \ln \rho)_S$ ($\approx 2/3$). The particular magnitudes of these parameters depend on the types of nuclear burning and on the temperature and density regime under consideration. Thus, the terms in Equation (33) always contribute positively to the work integral W. Physically, it can be understood as follows: In the compression phase, temperature and hence the nuclear energy generation rate are both systematically higher than in equilibrium so that matter gains thermal energy. During expansion, the nuclear energy generation rate drops below the equilibrium value and matter loses thermal energy. This particular phasing of energy gain and loss leads to a gradual increase of the perturbation amplitudes.

In the above discussion we assumed that the time scale of abundance changes by nuclear reactions was much longer than the pulsation time scale. Hence, equilibrium abundances of the involved chemical species could always be assumed. If the two time scales are comparable, however, additional perturbation equations must be supplied for each of the atomic species involved in the considered nuclear burning cycle (Ledoux & Walraven 1958, Unno et al 1989). The study of Kawaler (1988) provides an example of the influence of phase delays in generating and destroying chemical elements during a pulsational cycle on the destabilization of H-shell burning white dwarfs.

3.3.2 κ-MECHANISM The second term on the right-hand side of Equation (32) can be expressed as

$$-\int_0^M \frac{\delta T_r}{T}\delta\left(\frac{1}{\rho}\nabla\cdot\mathbf{F}_\mathrm{R}\right)_r dM_r$$
$$\propto \int_0^R \left(\frac{\delta T_r}{T}\right)^2 \frac{d}{dr}\left[\left(\kappa_T + \frac{\kappa_\rho}{\Gamma_3 - 1}\right)L_\mathrm{R}\right] dM_r + \ldots \tag{34}$$

where $\kappa_T = (\partial \ln \kappa/\partial \ln T)_\rho$ and $\kappa_\rho = (\partial \ln \kappa/\partial \ln \rho)_T$. This integral describes the action of the κ-mechanism. If the radiative luminosity L_R is constant as in a radiative envelope, a region with

$$\frac{d}{dr}\left(\kappa_T + \frac{\kappa_\rho}{\Gamma_3 - 1}\right) > 0 \tag{35}$$

helps to drive pulsation. When condition (35) is satisfied, the opacity perturbation increases outward so that the radiative luminosity is blocked in the compression phase of pulsation. Hence, the zone gains thermal energy in the compression phase and it loses thermal energy in the expansion phase.

The κ-mechanism, due to partial ionization of H and He I and/or He II, is responsible for pulsations of the stars in the classical instability strip (see Figure 1). The red variables probably gain pulsation energy from the partial ionization of hydrogen. Carbon/oxygen partial ionization is believed to be responsible for the oscillations of the hot central stars of planetary nebulae and of the DO white dwarfs. The details of the applications to classes of pulsating stars will be provided in Part 2 of this review.

Recent recalculations of astrophysical opacities had a major impact on stellar pulsation theory. The new generation of Rosseland opacity-means, based on state-of-the-art microphysics, is described in Rogers & Iglesias (1992), in Iglesias et al (1992) for the OPAL project, and in Seaton et al (1994) for the OP project. The calculations show a significant enhancement over the old Los Alamos data (up to a factor of about 3 depending on the density) of the Rosseland mean opacity at temperatures between about 100,000 and 300,000 K (see Figure 4). This new feature is referred to often as the "Z-bump" because it is caused by intra–M-shell transitions mainly in Fe and by fine-structure transitions in Mg, Cr, and Ni. The results obtained from OPAL and OP agree very satisfactorily, considering that the two projects worked completely independent of each other and used different physical descriptions for the plasma.

Based on the new opacity data, one could either eventually identify driving mechanisms (β Cepheids and B-type pulsators) or improve values for periods and period ratios. Again we refer to Part 2 for detailed discussions.

The third term on the right-hand side of Equation (32) describes the influence of the perturbed convective flux. Since convection in stars is turbulent, a correct modeling of this term is very difficult (Baker 1987, Unno & Xiong 1993). The uncertain convection description enters also through the momentum equation (7). Most calculations neglect any perturbation of the convective flux and also neglect the influence of turbulent pressure fluctuations. Such an approach produces reasonable results for sufficiently hot stars with weak convection zones. For example, the blue edge of the Cepheid instability strip and the β-Cephei variables can be recovered satisfactorily. However, to obtain the red edges of instability regions and to study the pulsations of red variables such as the Mira variables a proper treatment of pulsation-convection interaction is indispensable. No commonly agreed upon description has, however, yet emerged.

3.3.3 STOCHASTIC EXCITATION Stochastic excitation of nonradial oscillations occurs in connection with turbulent flows. The effect of turbulence appears as a source term in the wave equation (even in the adiabatic approximation). The momentum equation for wave and turbulent motions can be written as

$$\frac{\partial \mathbf{v}}{\partial t} + \mathbf{v} \cdot \nabla \mathbf{v} = \frac{1}{\rho} \nabla p - \nabla \psi,$$

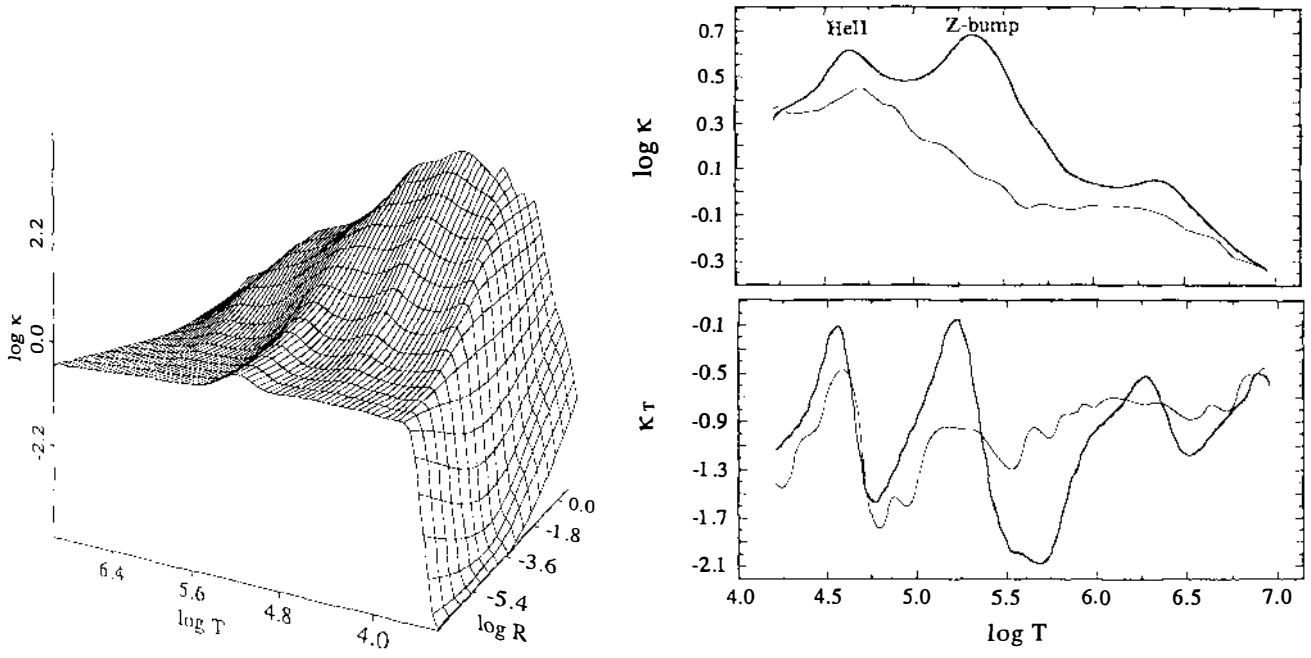

Figure 4 (*Left*) The "opacity mountain" from OP project data for $X = 0.7$, $Y = 0.28$. The independent variables are the logarithms of temperature T and $R \equiv \rho/(T/10^6\text{K})^3$. $\kappa_T = (\partial \ln \kappa/\partial \ln T)_\rho$. The new "Z-bump" feature appears as a prominent ridge around $\log T = 5.2$. (*Right*) Run of the opacity and of the important derivative κ_T through the interior, parameterized by the logarithm of the temperature, of a 12 $M_\odot$ main-sequence star model. The thin lines result from old Los Alamos Opacity Library data and the thick lines from OPAL data. Again, the Z-bump and its induced steep slope in κ_T are clearly visible.

where $\mathbf{v}$ includes the contributions of both oscillatory and turbulent motions. Subtracting the time-averaged part from the above equation, differentiating with respect to t, and using the adiabatic relation (12) for perturbed quantities, we obtain a wave equation

$$\frac{\partial^2 \mathbf{v}}{\partial t^2} + \mathrm{L}(\mathbf{v}) = -\frac{\partial}{\partial t}(\mathbf{v} \cdot \nabla \mathbf{v}) + \text{ other nonlinear terms}, \tag{36}$$

where L is a linear operator. The source term (right-hand side) of the wave equation is dominated by turbulent motion and hence has a stochastic character inherited from the turbulent eddies.

The stochastic excitation of p-mode pulsations is physically equivalent to acoustic noise generation by turbulent eddies. This problem has been extensively investigated by Lighthill (1952) for isotropic homogeneous turbulence and by Stein (1968) for a stratified convective layer. Goldreich & Keeley (1977) were the first to consider stochastic excitation as a viable driving mechanism of the solar five-minute oscillations.

Information on the damping and excitation rates of the solar five-minute oscillations is obtained from "line" widths in the oscillation-frequency spectrum and from the power in each oscillation mode as a function of frequency. Such data were presented by Libbrecht (1988). Although recent theoretical considerations by Osaki (1990), Balmforth (1992), and Goldreich et al (1994) reproduced roughly observed properties, many uncertainties remain in the theoretical approaches. For example, Goldreich et al (1994) claim that the entropy fluctuations expected in turbulent eddies [which are not included in Equation (36)] play the dominant role for stochastic excitation, while Osaki (1990) argues that the main contribution comes from the turbulent stress on the right-hand side of Equation (36).

The uncertainties result mainly from our poor understanding of the properties of turbulent convection in stars. The efficiency of stochastic excitation is very sensitive to the convective velocity near the outer boundary, where the characteristic velocity of energy-bearing eddies is maximum and the temperature gradient departs significantly from the adiabatic one. Accurate observational data expected to become available in the near future from the solar five-minute oscillations will help improve our understanding of the physical properties of turbulence in the outer part of the solar convection zone.

3.3.4 EXCITATION BY OSCILLATORY CONVECTION Linear convective instability in a nonrotating spherical star is understood in terms of g^--modes (for which $\sigma^2 < 0$), which occur whenever a star has a region with $N^2 < 0$. In a rotating star, some convective modes tend to be stabilized (section 14.5 in Tassoul 1978). Also, as discussed in Section 3.2.4, in a rotating star g^--modes have real parts proportional to $m\Omega$. In other words, oscillatory overstable g^--modes can exist in rotating stars. Osaki (1974) suggested that β Cepheid pulsations

are excited by a resonance between a p-mode and an overstable g^--mode of a rotating star. Later, Lee & Saio (1986, 1987) showed numerically that oscillatory convective modes couple with high-order g^+-modes of the envelope to form an overstable low-frequency (in the corotating frame) oscillation mode. Such a mode has large oscillation amplitude both in the convective core and in the envelope. Lee (1988) confirmed that the same phenomenon also occurs in differentially rotating stars.

If the coupling between core and envelope is artificially neglected, the involved oscillatory convective mode turns neutrally stable in the adiabatic approximation (Lee & Saio 1989), i.e. the convective mode is completely stabilized by the effect of rotation. Hence, it is the *coupling* between an oscillatory (stabilized) convective mode in the core and a g^+-mode in the envelope that results in an overstable oscillation mode. This interesting phenomenon was explained as follows: Lee & Saio (1990b) showed the oscillatory convective modes to have negative energy and the ordinary g^+-modes to have positive energy. When a negative energy mode couples with a positive energy one, energy can flow from the negative energy mode to the positive energy mode and the amplitudes of both parts increase. The energy reservoir being tapped in this case is the stars' rotation. Such overstable oscillation modes may be considered as an explanation of the short-period light variation of Be stars (Balona 1990) and as the driving mechanism for the very slow oscillations in the atmosphere of Jupiter (Lee & Saio 1990a).

3.3.5 TIDAL INTERACTION The tidal interaction between binary stars can be studied in the framework of forced nonradial oscillations on the individual components of the system. If the binary orbit is close to circular and the rotation of the components is synchronous with the orbital motion, then the tidal deformation becomes stationary and induces an *equilibrium tide* on the stars, which remain always in hydrostatic equilibrium. For nonradial oscillations in stationary, tidally deformed stars see Chandrasekhar & Lebovitz (1963), Denis (1972), Saio (1981), and Martens & Smeyers (1986). Perdang (1988) performed interesting ray tracings, appropriate for geometrical acoustics, in deformed stellar configurations to search for spatially chaotic solutions.

If, however, the orbit is elliptic, stellar rotation is not synchronous, or the rotation axis of the stars is not perpendicular to the binary orbit, then the tidal force becomes time dependent and induces fluid motion in a coordinate frame comoving with the star. Under such circumstances the induced *dynamical tide* can be described as a forced nonradial oscillation. The modified nonradial dynamics of a rotating star under the influence of a time-dependent external gravitational potential $U_{\rm comp}$ can be written as

$$-(\sigma + m\Omega)^2\boldsymbol{\xi} + 2\mathrm{i}(\sigma + m\Omega)\boldsymbol{\Omega}\times\boldsymbol{\xi} + \boldsymbol{\Omega}\times(\boldsymbol{\Omega}\times\boldsymbol{\xi}) = -\mathcal{L}(\boldsymbol{\xi}) + \nabla U_{\rm comp}(r,\theta,\phi;t).$$

The external potential U_{comp} is usually expanded in terms of spherical harmonics that account for the geometrical properties of the binary orbit. Each spherical harmonic is additionally expanded in a Fourier series to approximate the time dependence of the gravitational field (see Zahn 1977), which then leads to the theory of dynamical tides.

Cowling (1941) realized that low-frequency (free) eigenmodes of a binary component can enter into resonance with forced oscillation modes. Such resonances are believed to significantly influence circularization, synchronization, and apsidal-motion rates (Paploizou & Pringle 1980, Smeyers et al 1990) in binary stars through exchange of orbital and oscillation energy. Zahn (1966) found that dynamical tides can be damped by turbulent viscosity in convective stellar envelopes. For radiative envelopes, the nonadiabatic damping inherent in partial dynamic tides is believed to be responsible for producing significant torques in the stars (Zahn 1975, Savonije & Papaloizou 1983, Goldreich & Nicholson 1989) that tend to synchronize rotation with orbital motion. When it was realized that rotation influences the eigenfrequencies of g-modes and induces an additional mode spectrum (toroidal modes), rotation of the binary components was included in studies of forced oscillations, e.g. by Papaloizou & Pringle (1981) and Rocca (1982, 1987).

Alexander (1987, 1988) accounted self-consistently for the interaction between free oscillation modes of the binary components and the orbital motion in his perturbation-Hamiltonian approach. In this ansatz, the binary orbit is no longer kept fixed: It changes because of energy transfer from the binary orbit to normal modes of the stars.

3.4 *Strongly Nonadiabatic Pulsations*

Stellar pulsation can be considered, in its simplest formulation without complications by rotation, magnetic fields, etc, as a thermo-mechanical, coupled oscillator problem. A suggestive way of presenting the radial pulsation equations in this way can be found in section 7 of Gautschy & Glatzel (1990). (The formulation was motivated by the decomposition of normal modes suggested in Pesnell & Buchler 1986.) The coupling of the system depends on the ratio of the thermal (τ_{th}) to the dynamical time scale (τ_{dyn}) at a given location in the star. This ratio is typically large throughout most of a stellar envelope and drops below unity only for the outermost regions. Hence, nonadiabatic effects often influence the damping rate of an oscillation mode but the oscillation period, at least of low-order modes, is affected insignificantly. The quasi-adiabatic approximation of the stellar pulsation problem can yield satisfactory solutions under such circumstances.

Whenever the thermal time scale $\tau_{th} \approx 4\pi r^2 \rho \Delta r c_V T / L_r$ of a region with radial extension Δr of the star happens to become comparable to the sound-traveling time through that region ($\tau_{dyn} \approx \Delta r / c_s$), however, an efficient exchange of wave energy and thermal energy of the traversed stellar material

takes place. We know of types of pulsating stars for which the ratio τ_{th}/τ_{dyn} is small over a significant part of the propagation region of the pulsation modes (e.g. helium stars, very massive stars advanced on the AGB, some post-AGB stars). As can be seen from the definition of the thermal time scale, such stars have preferentially high luminosity-to-mass ratios. For such objects, the oscillation periods calculated fully nonadiabatically may differ significantly from the adiabatic ones. The growth/damping rates of perturbations can become significant compared with their oscillation frequencies. Under such circumstances the use of the work integral—which is based on the notion of a well-defined cycle in order to define appropriate time averages—becomes problematic. For an alternative discussion see Glatzel (1994).

It was also in stellar models with strongly nonadiabatic pulsations where the so-called strange modes were first encountered (Wood 1976, Cox et al 1980, Saio et al 1984). In modal diagrams additional modes were found to those expected from adiabatic considerations. The strange modes showed a deviating frequency behavior compared to the "regular" ones by crossing them when the control parameter of the model series varied. Actually, there was no real crossing occurring in the sense of a local degeneracy of frequencies, but two solutions of unfoldings were found (Gautschy & Glatzel 1990): either an "avoided crossing" or an "instability band" (see also Section 3.2.3). A detailed description of these properties can be found in Gautschy & Glatzel.

Zalewski (1992) demonstrated the effect of the particular formulation of the outer boundary conditions to the linear eigenvalue problem on the magnitude of the frequencies of the emerging strange modes when he calculated a series of low-mass supergiant models. He also emphasized the importance of strong nonadiabaticity in the stellar envelopes for strange modes to occur and attributed their existence to sufficiently strong and well-localized entropy perturbations in ionization zones. Another way of looking at strange modes is to consider them as being waves that are trapped in parts of the acoustic cavity of the stellar envelopes. Such a trapping can be induced by strong spatial gradients of those physical quantities that determine the acoustic cavity, and they can generate additional spectra when waves are accidentally able to develop an appropriate phase behavior to match boundary conditions. Despite recent efforts (Glatzel 1994), a fully satisfactory explanation of the strange modes has not yet been reached, partially due to the complexity of the fully nonadiabatic pulsation problem even in the linear approximation. Examining the physics behind the instabilities connected with strange modes remains a topic of active research. Strange-mode-like features have also been recovered in adiabatic radial oscillations of stars (Kiriakidis et al 1993, Gautschy 1993). Analyses of the adiabatic acoustic cavities indeed support the picture of partial trapping of waves to form additional oscillation spectra, which are then termed strange modes.

The different excitation possibilities for stellar pulsations presented in Sections 3.3 and 3.4 constitute the physical basis of Part 2 of this review. There we attempt, from the viewpoint of stellar evolution, to understand the observed properties of pulsating stars within this framework.

3.5 *Nonlinear Pulsations*

Actual stellar pulsations are inevitably nonlinear and analytic solutions are possible for very idealized systems (see Cox 1974) only. Most investigations of nonlinear pulsations rely on numerical analyses. Recently, some semi-analytical approaches to nonlinear pulsations were developed. For a recent review, see Buchler (1993).

Christy (1964) was the first to apply numerical hydrodynamic simulations to stellar pulsations. He considered the temporal behavior of a pulsating stellar envelope as an initial-value problem. For most classical pulsators, the growth time of the amplitude of the pulsation is much longer than its period. To get the limiting amplitude characteristics by direct hydrodynamic simulation, it is thus necessary to compute a large number of pulsation cycles. Stobie (1969) reduced the amount of computing time for such a project by artificially amplifying the amplitude. But even with this technique, a few dozen periods had to be followed before a Cepheid model arrived at its limit cycle. A different path to obtain strictly periodic pulsations was proposed by Baker & Sengbusch (1969). In their method, the structure of the stellar envelope is solved for iteratively at a number of phases of an appropriately estimated pulsation period. In this extended boundary-value approach, the pulsation period appears as an eigenvalue of the problem. The original method had numerical difficulties in the most superficial layers; these were overcome by modifications introduced by Stellingwerf (1974). His approach allowed for the evaluation of the stability of the nonlinear limit cycle (Floquet stability). Stellingwerf (1975) applied the method to RR Lyrae stars and showed that their linear stability behavior was insufficient to predict their final nonlinear behavior, in particular for the regions on the HR diagram where several modes are excited simultaneously. For example, inside the instability strip of RR Lyrae stars a region exists where both the fundamental and the first-overtone mode are excited simultaneously. Which pulsation mode is eventually selected by the star depends seemingly on the mode in which the star's pulsation is initiated (also known as the hysteresis effect).

Because nonlinear pulsation calculations require large amounts of computer time, the number of spatially distributed grid points is typically much smaller than what is used in linear analyses. For appropriate numerical resolution of important physical processes the distribution of the grid points is, however, crucial. In conventional hydrodynamical codes, grid points are attached to mass shells, i.e. to fixed Lagrangian coordinates. Lagrangian grids become inaccurate when physical variables vary rapidly and when such regions move

across different mass shells during a pulsation cycle. For example, the partial hydrogen-ionization zone or shock waves cause such problems. To avoid inaccuracies by steep, unresolved gradients of important physical quantities, adaptive-grid schemes were developed (Castor et al 1977). Aikawa & Simon (1983) wrote a computer code in which the temperature acts as the independent variable, at least throughout the partial hydrogen-ionization zone. This resulted in a numerically well-resolved driving region as the grid followed the ionization front during a pulsation cycle. Dorfi & Feuchtinger (1991) and Gehmeyr (1992a, b) opted for a more general scheme: The distribution of grid points is calculated together with the spatial structure of the stellar model at each time step. A delicate problem with non-Lagrangian grid points is, however, that advection errors of the grid can amount to a considerable fraction of the pulsation energy even if the relative error is kept very small. Deep in the interior, energy is much less than the internal energy; however, this is not the case far out in the envelope. In adaptive meshes, small errors can easily propagate through the grid and hence across the models and cause numerical difficulties at unexpected places.

At present, realistic nonlinear hydrodynamic codes are all one dimensional. Thus, only radial pulsations, devoid of any coupling with nonradial modes, can be simulated. Only Deupree (1974) attempted to simulate nonlinear, nonradial pulsations in β Cep stars with a two-dimensional nonlinear hydrodynamic code. For better physical insight into nonlinear dynamics of stellar pulsations a semi-analytic approach was developed in which the radial displacement is expanded in linear pulsation modes (Papaloizou 1973, Takeuti & Aikawa 1980, Perdang & Blacher 1984). Nonlinear coupling processes were included with a perturbation analysis by retaining second- and third-order amplitude terms (Vandakurov 1977, Dziembowski 1982, Buchler & Goupil 1984, Däppen & Perdang 1985). The velocity field is assumed to be a superposition of linear pulsation modes:

$$\mathbf{v} = \sum_k \left(A_k \mathbf{u}_k e^{i\sigma_k t} + A_k^* \mathbf{u}_k^* e^{-i\sigma_k t} \right),$$

where the $\mathbf{u}_k$ are velocity eigenfunctions of linear pulsation modes, the σ_k are the real parts of linear eigenfrequencies, and the A_k are time-dependent amplitudes (which include the effect of linear growth rates). An asterisk denotes the complex conjugate of a quantity. When the above form is substituted into the governing equation for the velocity, nonlinear terms generate contributions proportional to $\exp[i(\pm\sigma_k \pm \sigma_{k'})t]$ (second-order terms), $\exp[i(\pm\sigma_k \pm \sigma_{k'} \pm \sigma_{k''})t]$ (third-order terms), etc. As an example, consider a weakly nonlinear pulsation with frequency σ_1. For second-order terms to reproduce a temporal behavior comparable with the main pulsation the following resonance conditions should be satisfied: $\sigma_1 \approx \sigma_2 + \sigma_3$ or $\sigma_1 \approx 2\sigma_2$. Far from a resonance between second-order terms, third-order terms can still develop a time dependence of $\exp(\pm i\sigma_1 t)$. The resulting terms are then proportional to $|A_k|^2 A_1$ or $|A_k|^2 A_1^*$

for all values of k. Thus, such a case involves a large number of terms in general and is very laborious to treat analytically.

Consider a three-mode or two-mode resonance (coupling). We characterize the deviation from exact resonance by $\Delta\sigma = \sigma_1 - (\sigma_2 + \sigma_3)$ for a three-mode resonance, or by $\Delta\sigma = \sigma_1 - 2\sigma_2$ for a two-mode resonance. Multiplying the momentum equation by $\exp(-i\sigma_k t)$ ($k = 1, 2, 3$), integrating over the stellar volume, and averaging over a time scale longer than $1/\sigma_1$ but shorter than $1/\Delta\sigma$, we obtain equations governing the temporal evolution of the amplitudes, A_1, A_2, and A_3—the *amplitude equations* (Dziembowski 1982):

$$\frac{dA_1}{dt} = \kappa_1 A_1 + \epsilon H_1 A_2 A_3 e^{-i\Delta\sigma t},$$

$$\frac{dA_{2,3}}{dt} = \kappa_{2,3} A_{2,3} + H_{2,3} A_1 A_{3,2}^* e^{i\Delta\sigma t},$$

where $\epsilon = 1$ for three-mode resonances and $\epsilon = 0.5$ for two-mode resonances. The κ_k stand for linear growth rates and the H_k denote coupling constants. For example,

$$H_1 \propto \int Y_{\ell_1}^{m_1 *} Y_{\ell_2}^{m_2} Y_{\ell_3}^{m_3} \, d\Omega,$$

which are nonzero only when $m_1 = m_2 + m_3$ and $|\ell_2 - \ell_3| \leq \ell_1 \leq |\ell_2 + \ell_3|$ (Messiah 1962). This shows that a radial mode ($l_1 = m_1 = 0$) can couple with two nonradial modes with $\ell_2 = \ell_3$ and $m_2 = -m_3$. By such a coupling, a linearly overstable radial mode can excite two nonradial modes of lower frequencies (parametric resonance), or two linearly overstable nonradial modes can excite a radial mode of higher frequency (direct resonance). The possibility of excitation of pulsations through nonlinear coupling was first discussed in detail by Vandakurov (1977, 1979).

Results from amplitude-equation analyses are of importance for questions concerning the modal selection in variable stars such as in δ Scuti variables or in white dwarfs where many more unstable modes are calculated in linear analyses than are observed. Also, the amplitude-limitation mechanisms in low-amplitude pulsators such as δ Scuti stars are currently believed to be related to nonlinear mode coupling.

4. RELATIVISTIC PULSATIONS

The influence of relativity on stellar oscillations needs to be considered for very massive and/or very compact astronomical objects. Even when the structure of the object itself is not yet strongly influenced by general-relativistic effects, the perturbation of the dynamics of this structure may already be significantly affected. In contrast to pulsations in the Newtonian framework, in addition to the perturbation of the equilibrium configuration, the perturbation of space-time metric in which the object is embedded also needs to be included in the analysis.

Radial pulsation studies address mainly the *dynamical* stability properties of objects for which the quantity GM_*/c^2R_* is no longer small. For example, this applies to supermassive stars with masses above $10^4 M_\odot$, which were postulated to exist by Hoyle & Fowler (1963) to explain the properties of quasars. Chandrasekhar (1964) formulated the eigenvalue equations in the general-relativistic framework for radial perturbations of spherically symmetric fluid configurations in the adiabatic approximation. A self-adjoint differential equation can be derived for the displacement from equilibrium. All other quantities such as pressure, density, and metric coefficients can be deduced therefrom. With a few modifications in the occurring coefficients, the operator describing the boundary-value problem has the same mathematical properties as the one describing the Newtonian, adiabatic radial pulsation problem. In the post-Newtonian approximation (Chandrasekhar 1964), a slightly modified dynamical stability condition for adiabatic fluid motion was derived via a variational procedure:

$$3\langle\Gamma_1\rangle - 4 > \mathcal{K}\frac{2GM_*}{c^2R_*^2},$$

where $\mathcal{K}$ is a positive definite number (assuming values between 0.425 for an $n = 1$ and 1.125 for an $n = 3$ polytrope) and $\langle\Gamma_1\rangle$ denotes an appropriately defined spatial mean of the adiabatic exponent. The above form of the dynamical stability condition shows that general relativity has a destabilizing effect. The radii at which a dynamical instability occurs is usually significantly larger than the Schwarzschild radius of the object. Nonrotating supermassive stars above about $4 \times 10^5 M_\odot$ were found unstable due to purely relativistic effects.

Demaret (1975) took into account nonadiabatic effects and terms due to deviations from thermal equilibrium of quasi-statically contracting supermassive stars. In the post-Newtonian formalism, instabilities seem to set in via vibrational modes rather than through monotonically growing ones. The oscillatory contributions in the eigensolutions are due to relativistic corrections. Scuflaire (1976) stressed that adiabaticity is a poor approximation for describing the actual behavior of supermassive star models. At the onset of the relativity-induced instability the effects of secular and dynamical modes are so immersed that a clear distinction between them becomes futile (see also Osaki 1972, Demaret & Ledoux 1973).

For compact stars like white dwarfs and neutron stars (Thorne 1966, Shapiro & Teukolsky 1983) the constitutional relations such as the equation of state (for neutron stars), inverse β-decay (for iron white dwarfs), or pycnonuclear reactions (for carbon white dwarfs) strongly influence their constitution. The general-relativistic dynamic instability thus might not be the crucial factor determining the mass limits under these circumstances. For the pycnonuclear reaction rates there still are, however, considerable uncertainties (Salpeter & Van Horn 1969, Schramm & Koonin 1990, Ogata et al 1991). For massive

helium or carbon white dwarfs the efficiency of the pycnonuclear energy release at low densities might decide whether the stars can be prevented from contracting to the critical density ($\sim 2 \times 10^{10}$ g cm^{-3}) where the relativistic dynamical instability sets in.

Nonradial oscillations of relativistic objects are of interest as possible sources for gravitational-wave emission if the spherical degree $\ell \geq 2$. Hence, even in the adiabatic approximation where Newtonian stellar oscillations are purely oscillatory (i.e. $\sigma_I \equiv 0$) relativistic oscillations can give rise to complex eigensolutions with finite damping rates. Such modes are termed "quasi-normal modes" in the literature. The problem of completeness of quasi-normal modes was discussed in Price & Husain (1992). The quantitative treatment of nonradial, relativistic oscillations is much more involved than that of radial ones. In the nonradial problem, the perturbations of the metric coefficients can no longer be derived directly from the displacement fields for the matter. Thorne & Campolattoro (1967) proposed a fifth-order system of equations, which was later reduced to a nonsingular, and physically more intuitive, fourth-order system by Detweiler & Lindblom (1985). In the fourth-order system, two equations describe the dynamics of the matter and the other two the perturbation of the space-time metric. Ipser & Thorne (1973) provide an account of the early developments of the relativistic nonradial-oscillation formalism.

The very fact of a coupling of the two physical quantities—the fluid configuration of the astronomical body and the space-time metric—leads to the generation of a family of rather strongly damped eigenmodes (w-modes) in space-time, whose origins required substantial effort to explain. As the importance of relativity (essentially GM_*/c^2R_*) decreases, the w-modes increase their imaginary parts, which drift off to infinity in the Newtonian (uncoupled) limit (Kokkotas & Schutz 1992).

Although the equations given by Thorne & Campolattoro (1967) and Detweiler & Lindblom (1985) are suitable for describing p- and g-modes, they were found to be inappropriate for *numerically* calculating g-modes. McDermott et al (1983) introduced the concept of the "relativistic Cowling approximation," which reduced, through neglecting the Eulerian perturbation of the space-time metric, the problem to a system of equations for the dynamics of the fluid system only. Finn (1988) proved that, for the relativistic Cowling approximation, the same statements regarding the modal behavior of a star apply as in the Newtonian case.

Neutron star oscillations were proposed to explain quasi-periodic variability found in radio-pulsar and X-ray burster signals. The expositions of Van Horn (1980) and McDermott et al (1988) are informative sources on the observational background.

The theoretical evidence that neutron stars develop solid crusts close to their surfaces early in their evolution (Shapiro & Teukolsky 1983) allows for the

possibility of involved modal spectra of oscillations encountered in such objects. In addition to the well-known spheroidal p- and g-modes, shear modes also develop whose main restoring force is shear stress of the crust. Even in nonrotating stars the nonvanishing shear modulus of the crust is sufficient to lift the frequency degeneracy of the toroidal modes. McDermott et al (1988) studied the impressive phenomenology of oscillations of toroidal and spheroidal types in fluid-only as well as in three-component neutron-star models (fluid core, solid crust, and fluid surface regions) in the Cowling approximation. Schumaker & Thorne (1983) derived general relativistic equations facilitating the description of toroidal modes induced by possible solidified regions inside neutron stars. Contributions of nonvanishing shear moduli to even-parity (spheroidal) modes were included in the fully relativistic oscillation equations by Finn (1990).

In multicomponent neutron star models, the number of independent g-mode spectra is controlled by the number of separate fluid regions. In the three-component models two g-mode spectra occur: one defined in the surface region and one defined in the core of the neutron star. In addition to the shear modes (spheroidal and toroidal), which are essentially confined to the crustal region, interfacial modes also appear. These only have significant amplitudes very close to the fluid/solid and solid/fluid interfaces. McDermott et al (1988) and Carroll et al (1986) identified only one mode of interfacial type at each interface.

Even in isentropic neutron star models the degeneracy of the g-mode frequencies at zero can be lifted due to finite density jumps at locations of composition changes in the interior. The Baym, Pethik & Sutherland (1971) equation of state, for instance, predicts a number of first-order phase transitions in fully catalyzed matter. Finn (1987) studied g-modes at density discontinuities, applying his general relativistic "slow-motion approximation" to perfect fluid neutron star models with a simplified discontinuous equation of state. Strohmayer (1993) performed an analysis of the modal response to a density discontinuity in three-component neutron-star models employing a Newtonian Cowling approximation. Both authors agree that, depending on where the density discontinuity appears within the neutron star, the induced discontinuity modes may have frequencies comparable with those of g-modes generated by a finite entropy gradient in the star. If g-modes should ever be detected in neutron stars, the possible mode interactions between the two g-mode families might serve as a useful tool for diagnosing the equation of state.

In fully relativistic calculations, the damping of oscillation modes by gravitational-wave radiation has been calculated self-consistently (e.g. Thorne 1969, Lindblom & Detweiler 1983) in the form of a complex-valued boundary-eigenvalue problem for quadrupole f- and p-modes. From the derived damping times, of the order of tenths of seconds, it seems unlikely that such f- and p-modes can be directly observed in neutron stars. Other damping mechanisms, such as neutrino damping, electromagnetic radiation damping due to a

magnetic field frozen into the oscillating neutron star matter, nonadiabatic effects, or internal friction and viscosity were hitherto treated in a quasi-adiabatic approximation.

Carroll et al (1986) included strong magnetic fields into the pulsation analyses but for a simplified geometry, approximating in cylindrical symmetry the footing region of a dipole magnetic field on a neutron star. They recovered very interesting mode interactions involving Alfvénic modes generated by the frozen-in magnetic field of the neutron star and hydrodynamic modes, which were substantially modified by the presence of strong magnetic fields.

Superfluidity is not yet explicitly accounted for in the equations implemented in the stability analyses of neutron stars. Consequently, phenomena connected with particular properties of superfluids (such as vortex oscillations; Ruderman 1970) have not yet been investigated in a self-consistent manner.

Rotation not only lifts the m degeneracy but also couples spheroidal and toroidal modes. A first-order rotational perturbation ansatz for multicomponent, slowly rotating neutron star models by Strohmayer (1991) showed that the mixing of spheroidal and toroidal components in describing rotationally perturbed eigenfunctions modifies the damping of the modes. For example, in the nonrotating case, purely toroidal modes will gain spheroidal (and hence radial) components when rotationally perturbed; this then induces damping due to neutrino cooling or possibly gravitational-wave radiation, both of which are ineffective in a nonrotating model. But because rotation periods of neutron stars range from milliseconds to seconds, the approximation by a power-series expansion in Ω/ω (see Section 3.2.4) of the rotationally modified oscillation frequencies can fail for almost any kind of mode family. A reliable, general-purpose pulsation-rotation coupling scheme still needs to be developed.

It was realized by Chandrasekhar (1970), and shown to be a generic result by Friedman & Schutz (1978), that all rotating inviscid stars are subject to a secular instability due to gravitational-wave radiation. The critical rotation frequency Ω above which gravitational-radiation instability sets in is roughly proportional to $m^{-1/2}$, where m is the azimuthal order of the mode. For quasi-Newtonian stars in particular, the growth rate of the gravitational-wave instability is so small that essentially any kind of dissipation mechanism stabilizes the star. Viscous forces normally grow as the spatial gradients of the perturbations grow; hence, viscous dissipation grows with increasing degree m. Thus, large enough viscosity can stabilize rapidly rotating stars. For neutron stars, however, with their relativistic structure and the prevailing exotic physical conditions, it is not clear a priori whether viscosity indeed limits their rotation rates. Numerical methods to study sectorial modes in rapidly rotating neutron stars, solving the full eigenvalue problem for the rotating, Newtonian fluid configuration, were developed by Ipser & Lindblom (1990). First-order post-Newtonian corrections to the Newtonian frequencies in rotating

stellar models were recently provided by Cutler (1991) and Cutler & Lindblom (1992).

Calculations by Ipser & Lindblom (1991) indicated that for temperatures $\lesssim 10^7$K and $\gtrsim 5 \cdot 10^{10}$ K there is no way for gravitational-radiation instabilities (through an $\ell = +m$ mode) to develop before reaching the break-up rotation rate for a slightly aged neutron star that is rigidly rotating. Only for neutron stars rotating close to the break-up speed ($\approx 0.95 \times \Omega_{\rm crit}$) do $m = -\ell$ modes induce a viscosity-driven instability (Lindblom 1987). Due to the large uncertainties in describing quantitatively the physical conditions prevailing in compact objects it remains uncertain whether such stars can indeed be sources of gravitational radiation if heated up, as might happen, for example, during an accretion process or if such radiation escapes only during relaxation oscillations excited by an ensuing thermonuclear flash.

5. HYDROGEN-DEFICIENT STARS

Hydrogen-deficient stars are usually luminous, with luminosities between 10^3 and $10^4 L_\odot$, and have a very low H abundance in their spectra (typically $n_{\rm H}/n_{\rm He} \lesssim 10^{-4}$). Some of them are also C and O rich. The R CrB-like stars, having effective temperatures below $\approx 10^4$ K, show IR excesses possibly caused by dust envelopes, and they suffer spectacular luminosity drops of several magnitudes, which are attributed to dust condensations in the circumstellar envelopes. The extreme He (EHe) stars are typically hotter than 10^4 K and show abundance properties similar to those of R CrB stars except for the dust envelopes and the associated phenomena, which seem to be missing. The nomenclature for the different subgroups of hydrogen-deficient stars is far from consistently used in the literature. Reviews of many important aspects of these stars can be found in the *Proceedings of the IAU Colloquium No. 87* (Hunger et al 1986).

More than a dozen H-deficient stars are observed to exhibit semiregular photometric and radial-velocity variations. Due to the large range of effective temperatures the time scales of variability range from fractions of a day (V652 Her, 0.11 d) to tens of days (R CrB $\approx$ 40 d, RY Sgr $\approx$ 38 d; see Lawson et al 1990). For some of the stars secular period changes have been reported, but these are still controversial (Lombard & Koen 1993). The pulsation aspects of H-deficient stars were recently reviewed by Saio (1986, 1990).

The pulsation hypothesis explaining the variability of H-deficient stars is supported by the decrease of their periods with increasing $T_{\rm eff}$ (Saio & Jeffery 1988, Lawson et al 1990). For homologous stars at the same luminosity and with the same mass there is a strict linear relation between $\log P$ and $\log T_{\rm eff}$. All H-deficient stars show high L/M ratios, between 10^3 and 10^4.

The evolutionary state of the H-deficient stars is not known. Two scenarios that might account for the most stringent constraints are in discussion. Schönberner (1977) suggested helium stars to be remnants of post-AGB stars

with masses around 0.7 $M_\odot$. Mechanisms accounting for the complete removal of the hydrogen-rich envelope to produce chemical abundances compatible with those observed in H-deficient stars have not been found (Schönberner 1986). The presently favored scenario proposed by Webbink (1984) and Iben & Tutukov (1985) invokes the merging of He and C-O white-dwarf binaries as the origin of C-rich, H-deficient stars. The theory is still far from quantitative, and it is not clear if the production rate of such mergers within a Hubble time is sufficient to account for the observed number of H-deficient stars (see e.g. Renzini 1990; Iben 1991, his Section 13; Bragaglia et al 1990) and if the resulting masses are compatible with those derived from pulsation analyses. The observed H-deficient *binaries* (HdB) show all only weak carbon features. All observed EHe stars with a strong carbon signature in their spectra are, in contrast, single stars. Jeffery et al (1987) take these results as evidence supporting the double-degenerate merging scenario. The H-deficient binaries, on the other hand, are believed to be well understood in the framework of mass-transferring binary star evolution (Delgado & Thomas 1981).

An intriguing observational fact is the unusually broad temperature range over which H-deficient stars are found to be variable. The instability region extends at least from $\log T_{\rm eff} \approx 3.7$ to 4.4. However, the classical instability strip has its blue edge at about $\log T_{\rm eff} = 3.8$ (for $\log L/L_\odot = 4$). Many concepts used in connection with the classical pulsators are derived from adiabatic or quasi-adiabatic considerations and must be revised when dealing with H-deficient stars. Their high L/M ratio makes their envelopes highly nonadiabatic, which influences not only stability properties significantly but also the pulsation periods. For some time (see Saio et al 1984 and references therein) it has been known that in addition to the modes expected from adiabatic analyses, other oscillation modes are recovered in linear, nonadiabatic calculations that have no counterparts in the adiabatic approximation. These "strange modes" were identified as the sources of instability, especially at high temperatures by Gautschy & Glatzel (1990). The strange modes are also responsible for very complicated modal diagrams with crossing and interacting modes; such an intricate behavior of eigenmodes was previously known only from nonradial pulsations where different mode families can cross each other. Both radial modes and low-ℓ, low-order nonradial modes were found unstable (Glatzel & Gautschy 1992). Jeffery & Heber (1992) showed the existence of nonradial modes in a H-deficient star from its line profile variations. The width of the instability region recovered from the linear stability analyses is in good agreement with observations. A high enough L/M ratio (resulting in luminosities above about $5 \times 10^3\, L_\odot$ for the masses appropriate for H-deficient pulsations) seems to be a sufficient condition for the instabilities to occur. Below about 0.7 $M_\odot$ the instabilities disappear. The problem case of V652 Her, which lies at a low luminosity of about $10^3 L_\odot$, always resisted the modeling of its pulsational

instabilities with the old Los Alamos opacity data. Saio (1992) succeeded in finding unstable modes having periods in agreement with observations by using the new OPAL opacity tables. Saio's result was also sensitive to the assumed heavy element abundance, an aspect not essential in the more luminous H-deficient stars. Indeed, the destabilizing factor for V652 Her is the Z-bump in the new opacity data. Radial modes in all other H-deficient variables are, on the other hand, excited by the influence of the He ionization zone, which not only destabilizes the modes but also traps them efficiently in the outermost layers and reduces radiative damping. A fully consistent understanding of the working of strange modes, in particular of their instabilities, is not yet available (see also Section 3.4). An important ingredient for the occurrence of strange modes, deduced from numerical calculations, is a sufficiently high L/M ratio. Saio & Jeffery (1988) concluded that the nonvariable EHe stars tend toward smaller L/M values than do the variable ones. Not understood is the fact that the visible components in HdB variables have systematically higher masses, deduced from pulsation analyses, than the single H-deficient stars.

The nonlinear pulsation simulations of H-deficient stars by Saio & Wheeler (1985) (for earlier attempts see the references therein) did not show limit cycles: For the very cool stellar models at around $\log T_{\rm eff} = 3.7$, the amplitudes grew without bound. The hotter models relaxed into (rather noisy) limit cycles, but the light amplitudes were significantly higher than those observed for these stars. Fadeyev (1990) extended the model grid for H-deficient stars to temperatures exceeding 10^4 K. For models with $L/M > 10^4$ he found unstable modes at very high effective temperatures to be very much in agreement with the predictions from linear theory. Fadeyev's simulations also suffered from light amplitudes that were too large; however, these decreased at higher effective temperatures. Some observations hint at the possibility that a finite-amplitude pulsation can trigger the major luminosity drops of R CrB stars. Recently, Lawson et al (1992) found that V852 Cen always starts its luminosity descents at approximately the same pulsation phase. For the same star, Clayton et al (1993) found that dust formation close to the surface occurs at the pulsation phase of maximum light.

ACKNOWLEDGMENTS

Easy access to the excellently equipped library at ESO headquarters proved indispensable for writing this exposition. The MOSAIC version of the ADS abstract service allowed for an efficient tracking down of references that might have been missed otherwise. JR Garcia and coworkers provided us with their database of variable stars in the lower instability strip. NH Baker succeeded in transforming the content of the manuscript into a comprehensible language and in eliminating misconceptions. AG obtained partial financial support from the Swiss National Science Foundation.

Literature Cited

The following abbreviations of conference proceedings are used in the text and in the list of references:

Bo90: *Confrontation between Stellar Pulsation and Evolution, ASP Conf. Ser.* Vol. 11, ed. C Cacciari, G Clementini (1990). San Francisco: Astron. Soc. Pac.

Buda88: *Multimode Stellar Pulsations,* ed. G Kovács, L Szabados, B Szeidl. Budapest: Kultura (1988)

ESO90: *ESO Workshop on Rapid Variability of OB-Stars: Nature and Diagnostic Value,* ed. D Baade. Garching: ESO (1991)

GONG92: *Seismic Investigation of the Sun and Stars, ASP Conf. Ser.* Vol. 42, ed. TM Brown (1993). San Francisco: Astron. Soc. Pac.

ITS92: *Inside the Stars, IAU Colloq. 137, ASP Conf. Ser.* Vol. 40, ed. WW Weiss, A Baglin (1993). San Francisco: Astron. Soc. Pac.

PSSS: *Progress of Seismology of the Sun and Stars, Lect. Notes Phys. 367,* ed. Y Osaki, H Shibahashi. New York: Springer-Verlag (1990)

Aerts C, De Pauw MD, Waelkens C. 1992. *Astron. Astrophys.* 266:294–306

Aikawa T, Simon NR. 1983. *Ap. J.* 273:346–54

Aizenman ML, Smeyers P, Weigert A. 1977. *Astron. Astrophys.* 58:41–46

Alexander ME. 1987. *MNRAS* 227:843–61

Alexander ME. 1988. *MNRAS* 235:1367–83

Baglin A, Weiss WW, Bisnovatyi-Kogan G. 1993. In ITS92, pp. 758–60

Baker NH. 1987. In *Physical Processes in Comets, Stars and Active Galactic Nuclei,* ed. W Hillebrandt, E Meyer-Hofmeister, H-C Thomas, pp. 105–24. New York: Springer-Verlag

Baker NH, Kippenhahn R. 1962. *Z. Astrophys.* 54:114–51

Baker NH, Kippenhahn R. 1965. *Ap. J.* 142:868–89

Baker NH, Sengbusch Kv. 1969. *Mitt. Astron. Ges.* 27:162–67

Balmforth NJ. 1992. *MNRAS* 255:639–49

Balona LA. 1986a. *MNRAS* 219:111–29

Balona LA. 1986b. *MNRAS* 220:647–56

Balona LA. 1990. *MNRAS* 245:92–100

Baym G, Pethick C, Sutherland P. 1971. *Ap. J.* 170:299–317

Belmonte JA, Roca Cortés T, Vidal I, Schmider FX, Michel E, et al. 1993, In ITS92, pp. 739–41

Bernstein IB, Brookshaw L, Fox PA. 1992, *J. Comp. Phys.* 98:269–84

Beyer HR, Schmidt BG. 1994. *Astron. Astrophys.* In press

Bragaglia A, Greggio L, Renzini A, D'Odorico S. 1990. *Ap. J. Lett.* 365:L13–17

Brown TM, Gilliland RL. 1994. *Annu. Rev. Astron. Astrophys.* 32:37–82

Brown TM, Christensen-Dalsgaard J, Weibel-Mihalas B, Gilliland RL. 1994. *Ap. J.* 427:1013–34

Buchler JR. 1993. *Astrophys. Space Sci.* 210:9–31

Buchler JR, Goupil M-J. 1984. *Ap. J.* 279:394–400

Cairns RA. 1979. *J. Fluid Mech.* 92:1–14

Carroll BW, Zweibel EG, Hansen CJ, McDermott PN, Savedoff MP, et al. 1986. *Ap. J.* 305:767–83

Castor JI, Davies CG, Davison DK. 1977. *Los Alamos Rep. LA-6664*

Chandrasekhar S. 1964. *Ap. J.* 140:417–33

Chandrasekhar S. 1970. *Ap. J.* 161:561–69

Chandrasekhar S, Lebovitz NR. 1963. *Ap. J.* 137:1172–84

Christy RF. 1964. *Rev. Mod. Phys.* 36:555–71

Clayton GC, Lawson WA, Whitney BA, Pollaco DL. 1993. *MNRAS* 264:L11–16

Clemens JC, Nather RE, Winget DE, Robinson EL, Wood MA, et al. 1992. *Ap. J.* 391:773–83

Cowling TG. 1941. *MNRAS* 101:367–75

Cox JP. 1974. Rep. Prog. Phys. 37:563–698

Cox JP. 1980. *Theory of Stellar Pulsation.* Princeton: Princeton Univ. Press

Cox JP, King DS, Cox AN, Wheeler JC, Hansen CJ, Hodson SW. 1980. *Space Sci. Rev.* 27:529–35

Cox JP, Whitney C. 1958. *Ap. J.* 127:561–72

Cutler C. 1991. *Ap. J.* 374:248–54

Cutler C, Lindblom L. 1992. *Ap. J.* 385:630–41

Däppen W, Perdang J. 1985. *Astron. Astrophys.* 151:174–88

Delgado AJ, Thomas H-C. 1981. *Astron. Astrophys.* 96:142–45

Demaret J. 1975. *Mem. Soc. R. Sci. Liège,* Colloq. 8, 6e Ser. 8:161–72

Demaret J, Ledoux P. 1973. *Astron. Astrophys.* 23:111–16

Denis J. 1972. *Astron. Astrophys.* 20:151–55

Detweiler SL, Lindblom L. 1985. *Ap. J.* 292:12–15

Deupree RG. 1974. *Ap. J.* 194:393–401

Dorfi EA, Feuchtinger MU. 1991. *Astron. Astrophys.* 249:417–27

Duerbeck HW, Seitter WC. 1982. In *Landolt-Börnstein, New Series,* ed. K Schaifers, HH Voigt, VI/2b:197–268 Berlin: Springer-Verlag

Dziembowski WA. 1982. *Acta Astron.* 32:147–71

Dziembowski WA, Goode PR. 1992. *Ap. J.*

394:670–87
Fadeyev YuA. 1990. *MNRAS* 244:225–32
Finn LS. 1987. *MNRAS* 227:265–93
Finn LS. 1988. *MNRAS* 232:259–75
Finn LS. 1990. *MNRAS* 245:82–91
Friedman JL, Schutz BF. 1978. *Ap. J.* 222:281–96
Gautschy A. 1992. *Astron. Astrophys.* 260:175–82
Gautschy A. 1993. *MNRAS* 265:340–46
Gautschy A, Glatzel W. 1990. *MNRAS* 245:597–613
Gehmeyr M. 1992a. *Ap. J.* 399:265–71
Gehmeyr M. 1992b. *Ap. J.* 399:272–83
Gilliland RL, Brown TM. 1988. *Publ. Astron. Soc. Pac.* 100:754–65
Gilliland RL, Brown TM, Duncan DK, Suntzeff NB, Lockwood GW, et al. 1991. *Astron. J.* 101:541–61
Glatzel W. 1987. *MNRAS* 228:77–100
Glatzel W. 1994. *MNRAS* 271:66–74
Glatzel W, Gautschy A. 1992. *MNRAS* 256:209–18
Goldreich P, Keeley DA. 1977. *Ap. J.* 212:243–51
Goldreich P, Murray N, Kumar P. 1994. *Ap. J.* 424:466–79
Goldreich P, Nicholson PD. 1989. *Ap. J.* 342:1079–84
Goode PR, Thompson MJ. 1992. *Ap. J.* 395:307–15
Goosens M. 1972. *Astrophys. Space Sci.* 16:386–404
Goosens M, Smeyers P, Denis J. 1976. *Astrophys. Space Sci.* 39:257–72
Gough DO, Thompson MJ. 1990. *MNRAS* 242:25–55
Gough DO, Toomre J. 1991. *Annu. Rev. Astron. Astrophys.* 29:627–84
Hansen CJ. 1972. *Astron. Astrophys.* 19:71–75
Hatzes AP, Kürster M. 1994. *Astron. Astrophys.* 285:454–58
Howell SB, ed. 1992. *Astronomical CCD Observing and Reduction Techniques,* ASP Conf. Ser. Vol. 23. San Francisco: Astron. Soc. Pac.
Hoyle F, Fowler WA. 1963. *MNRAS* 125:169–76
Hunger K, Schönberner D, Kameswara Rao N, eds. 1986. *Hydrogen Deficient Stars and Related Objects,* ASSL Vol. 128. Dordrecht: Reidel
Iben I Jr. 1991. *Ap. J. Suppl.* 76:55–114
Iben I Jr, Tutukov AV. 1985. *Ap. J. Suppl.* 58:661–710
Iglesias CA, Rogers FJ, Wilson BG. 1992. *Ap. J.* 397:717–28
Ipser JR, Lindblom L. 1990. *Ap. J.* 355:226–40
Ipser JR, Lindblom L. 1991. *Ap. J.* 373:213–21
Ipser JR, Thorne KS. 1973. *Ap. J.* 181:181–82
Jeffery CS, Heber U. 1992. *Astron. Astrophys.* 260:133–50
Jeffery CS, Drilling JS, Heber U. 1987. *MNRAS* 226:317–39
Jones PW, Pesnell WD, Hansen CJ, Kawaler SD. 1989. *Ap. J.* 336:403–8
Kawaler SD. 1988. *Ap. J.* 334:220–28
Kiriakidis M, Fricke KJ, Glatzel W, 1993. *MNRAS* 264:50–62
Kjeldsen H, Frandsen S. 1992. *Publ. Astron. Soc. Pac.* 104:413–34
Kokkotas KD, Schutz BF. 1992. *MNRAS* 255:119–28
Kovetz A. 1966. *Ap. J.* 146:462–70
Landau LD, Lifschitz EM. 1981. *Mechanik.* Berlin: Akademie
Lawson WA, Cottrell PL, Kilmartin PM, Gilmore AC. 1990. *MNRAS* 247:91–117
Lawson WA, Cottrell PL, Gilmore AC, Kilmartin PM. 1992. *MNRAS* 256:339–48
Ledoux P, Simon R. 1957. *Ann. Astrophys.* 20:185–95
Ledoux P, Walraven Th. 1958. *Handbuch der Physik,* ed. S Flügge, LI:353–604. Berlin: Springer-Verlag.
Lee U. 1988. *MNRAS* 232:711–24
Lee U, Saio H. 1986. *MNRAS* 221:365–76
Lee U, Saio H. 1987. *MNRAS* 225:643–51
Lee U, Saio H. 1989. *MNRAS* 237:875–901
Lee U, Saio H. 1990a. *Ap. J. Lett.* 359:L29–32
Lee U, Saio H. 1990b. *Ap. J.* 360:590–603
Libbrecht KG. 1988. *Ap. J.* 334:510–16
Lighthill MJ. 1952. *Proc. R. Soc. London Ser. A* 211:564–87
Lindblom L. 1987. *Ap. J.* 317:325–32
Lindblom L, Detweiler SL. 1983. *Ap. J. Suppl.* 53:73–92
Lombard F, Koen C. 1993. *MNRAS* 263:309–13
Lynden-Bell D, Ostriker JP. 1967. *MNRAS* 136:293–310
Martens L, Smeyers P. 1986. *Astron. Astrophys.* 155:211–26
McDermott PN, Van Horn HM, Hansen CJ. 1988. *Ap. J.* 325:725–48
McDermott PN, Van Horn HM, Scholl JF. 1983. *Ap. J.* 268:837–48
Messiah A. 1962. *Quantum Mechanics,* pp. 1056. Amsterdam: North-Holland
Mosser B, Mékarnia D, Maillard JP, Gay J, Gautier D, Delache P. 1993. *Astron. Astrophys.* 267:604–22
Nasiri S, Sobouti Y. 1989. *Astron. Astrophys.* 217:127–36
Nather RE, Winget DE, Clemens JC, Hansen CJ, Hine BP. 1990. *Ap. J.* 361:309–17
Noyes RW, Brown TM, Horner S, Korzennik S, Nisenson P. 1993. In GONG92, pp.485–88
Ogata S, Iyetomi H, Ichimaru S. 1991. *Ap. J.* 372:259–66
Osaki Y. 1971. *Publ. Astron. Soc. Jpn.* 23:485–502
Osaki Y. 1972. *Publ. Astron. Soc. Jpn.* 24:537–43
Osaki Y. 1974. *Ap. J.* 189:469–77
Osaki Y. 1975. *Publ. Astron. Soc. Jpn.* 27:237–58

Osaki Y. 1990. In PSSS, pp. 75–86
Papaloizou JCB. 1973. *MNRAS* 162:143–68
Papaloizou J, Pringle JE. 1978. *MNRAS* 182:423–42
Papaloizou J, Pringle JE. 1980. *MNRAS* 193:603–15
Papaloizou J, Pringle JE. 1981. *MNRAS* 195:743–53
Perdang J. 1988. In Buda88, pp. 209–63
Perdang J, Blacher S. 1984. *Astron. Astrophys.* 136:263–81
Pesnell WD, Buchler JR, 1986. *Ap. J.* 303:740–48
Pottasch EM, Butcher HR, van Hoesel FHJ. 1992. *Astron. Astrophys.* 264:138–46
Price RH, Husain V. 1992. *Phys. Rev. Let.* 68:1973–76
Provost J, Berthomieu G, Rocca A. 1981. *Astron. Astrophys.* 94:126–33
Renzini A. 1990. In Bo90, pp. 549–56
Ritter A. 1879. *Ann. Phys. Chem. Neue Folge* 8:157–83
Rocca A. 1982. *Astron. Astrophys.* 111:252–54
Rocca A. 1987. *Astron. Astrophys.* 175:81–90
Rogers FJ, Iglesias CA. 1992. *Ap. J. Suppl.* 79:507–68
Rosseland S. 1949. *The Pulsation Theory of Variable Stars.* Oxford: Oxford Univ. Press
Roxburgh IW, Vorontsov SV. 1994a. *MNRAS* 267:297–302
Roxburgh IW, Vorontsov SV. 1994b. *MNRAS* 268:143–58
Ruderman MA. 1970. *Nature* 225:619–20
Saio H. 1981. *Ap. J.* 244:299–315
Saio H. 1986. In *Hydrogen Deficient Stars and Related Objects,* ed. K Hunger, D Schönberner, N Kameswara Rao, ASSL Vol. 128, pp. 425–38. Dordrecht: Reidel
Saio H. 1990. In Bo90, pp. 557–65
Saio H. 1992. *MNRAS* 258:491–96
Saio H, Jeffery CS. 1988. *Ap. J.* 328:714–25
Saio H, Lee U. 1991. In ESO90, pp. 293–302
Saio H, Wheeler JC. 1985. *Ap. J.* 295:38–42
Saio H, Wheeler JC, Cox JP. 1984. *Ap. J.* 281:318–36
Salpeter EE, Van Horn HM. 1969. *Ap. J.* 155:183–202
Savonije GJ, Papaloizou J. 1983. *MNRAS* 203:581–93
Seaton MJ, Yan Y, Mihalas D, Pradhan AK. 1994. *MNRAS* 266:805–29
Schönberner D. 1977. *Astron. Astrophys.* 57:437–41
Schönberner D. 1986. In *Hydrogen Deficient Stars and Related Objects,* ed. K Hunger, D Schönberner, N Kameswara Rao, ASSL Vol. 128, pp. 471–80. Dordrecht: Reidel
Schramm SS, Koonin SE. 1990. *Ap. J.* 365:296–300
Schumaker BL, Thorne KS. 1983. *MNRAS* 203:457–89
Scuflaire R. 1976. *Astrophys. Space Sci.* 43:375–95
Shapiro SL, Teukolsky SA. 1983. *Black Holes, White Dwarfs and Neutron Stars.* New York: Wiley
Shibahashi H. 1979. *Publ. Astron. Soc. Jpn.* 31:87–104
Shibahashi H, Osaki H. 1976. *Publ. Astron. Soc. Jpn.* 28:199–214
Shibahashi H, Takata M. 1993. *Publ. Astron. Soc. Pac.* 45:617–41
Smeyers P. 1984. In *Theoretical Problems in Stellar Stability and Oscillations, 25th Liège Int. Astrophys. Colloq.,* ed. A Noels, M Gabriel, pp. 68–91
Smeyers P, Tassoul M. 1987. *Ap. J. Suppl.* 65:429–49
Smeyers P, van Hout M, Ruymaekers E, Polfliet R. 1990. *Astron. Astrophys.* 248:94–104
Stein RF. 1968. *Sol. Phys.* 2:385–432
Stellingwerf RF. 1974. *Ap. J.* 192:139–44
Stellingwerf RF. 1975. *Ap. J.* 195:441–66
Stobie RS. 1969. *MNRAS* 144:461–84
Strohmayer TE. 1991. *Ap. J.* 372:573–91
Strohmayer TE. 1993. *Ap. J.* 417:273–78
Takata M, Shibahashi H. 1994. *Publ. Astron. Soc. Jpn.* 46:301–14
Takeuti M, Aikawa T. 1980. *MNRAS* 192:697–707
Tassoul J-L. 1978. *Theory of Rotating Stars.* Princeton: Princeton Univ. Press
Tassoul M. 1980. *Ap. J. Suppl.* 43:469–90
Tassoul M. 1990. *Ap. J.* 358:313–27
Thorne KS. 1966. In *High Energy Astrophysics, Proc. Int. School Physics Enrico Fermi, Course 35,* ed. L Gratton, pp. 166–280. New York: Academic
Thorne KS. 1969. *Ap. J.* 158:1–16
Thorne KS, Campolattoro A. 1967. *Ap. J.* 149:591–611
Unno W, Osaki Y, Ando H, Saio H, Shibahashi H. 1989. *Nonradial Oscillations of Stars.* Tokyo: Univ. Tokyo Press. 2nd ed.
Unno W, Xiong D-R. 1993. *Astrophys. Space Sci.* 210:77–81
Vandakurov YuV. 1968. *Sov. Astron.* 11:630–38
Vandakurov YuV. 1977. *Sov. Astron. Lett.* 3:249–51
Vandakurov YuV. 1979. *Sov. Astron.* 23:421–25
Van Hoolst T, Smeyers P. 1991. *Astron. Astrophys.* 248:647–55
Van Horn HM. 1980. *Ap. J.* 236:899–903
Vogt SS, Penrod GD. 1983. *Ap. J.* 275:661–82
Vorontsov SV. 1992. *Sov. Astron.* 35:400–8
Webbink RF. 1984. *Ap. J.* 277:355–60
Wood PR. 1976. *MNRAS* 174:531–39
Xiong D-R. 1981. *Acta Astron. Sinica* 22:350–56
Zahn J-P. 1966. *Ann. Astrophys.* 29:489–506
Zahn J-P. 1975. *Astron. Astrophys.* 41:329–44
Zahn J-P. 1977. *Astron. Astrophys.* 57:383–94
Zalewski J. 1992. *Publ. Astron. Soc. Jpn.* 44: 27–43
Zhevakhin SA. 1963. *Annu. Rev. Astron. Astrophys.* 1:367–400